ISTANBUL TECHNICAL UNIVERSITY ★ GRADUATE SCHOOL OF SCIENCE ENGINEERING AND TECHNOLOGY

MODELING AND DEVELOPMENT OF PIEZOELECTRIC BASED TACTILE SENSORS

M.Sc. THESIS

Farshad HAMEDI BAZZAZ

Department of Mechanical Engineering

System Dynamics and Control

DECEMBER 2017

ISTANBUL TECHNICAL UNIVERSITY ★ GRADUATE SCHOOL OF SCIENCE ENGINEERING AND TECHNOLOGY

MODELING AND DEVELOPMENT OF PIEZOELECTRIC BASED TACTILE SENSORS

M.Sc. THESIS

Farshad HAMEDI BAZZAZ
(503151621)

Department of Mechanical Engineering

System Dynamics and Control

Thesis Advisor: Prof. Dr.Şeniz Ertuğrul

DECEMBER 2017

İSTANBUL TEKNİK ÜNİVERSİTESİ ★ FEN BİLİMLERİ ENSTİTÜSÜ

DOKUNSAL PİEZOELEKTRİK ALGILAYICININ GELİŞTİRİLMESİ VE MODELLEMESİ

YÜKSEK LİSANS TEZİ

Farshad HAMEDI BAZZAZ
(503151621)

Makina Mühendisliği Anabilim Dalı

Sistem Dinamiiği ve Kontrol Programlı

Tez Danışmanı: Prof. Dr.Şeniz Ertuğrul

ARALIK 2017

Farshad HAMEDI BAZZAZ, a M.Sc. student of ITU Graduate School of Science Engineering and Technology 503151621 successfully defended the thesis entitled "MODELING AND DEVELOPMENT OF PIEZOELECTRIC BASED TACTILE SENSORS", which he/she prepared after fulfilling the requirements specified in the associated legislations, before the jury whose signatures are below.

Thesis Advisor :	**Prof. Dr.Şeniz Ertuğrul** Istanbul Technical University	.....
Jury Members :	**Prof. Dr.Şeniz Ertuğrul** Istanbul Technical University	.....
	Prof.Dr. Haydar Livatyalı Yıldız Technical University	.....
	Assoc. Prof. Dr. Pınar Boyraz Baykaş Istanbul Technical University	.....

Date of Submission : **17 November 2017**
Date of Defense : **15 December 2017**

To my beloved family and friends,

FOREWORD

This thesis is dedicated to my beloved family and friends who assisted me during my thesis research.

In the beginning, I would like to express my sincere gratitude to my advisor Prof. Dr. Şeniz Ertuğrul, my dear professor, Prof. Dr. Ata Muğan and our project leader Dr. Merve Acer for their guidance and encouragement. Without their kind support, this work would not have been possible. Besides, I would like to appreciate my thesis committee for their invaluable guidance, ideas and feedbacks.

I also would like to thank Duygu Özyıldırım, Adnan Furkan Yıldız, Arsalan Bayat Makoo, Uğurcan Sarı, Amir Mehrabi, Deniz Ezgi Gülmez, Ahmet Semih Ertürk and all of my friends in Mechatronics Education and Research Center for their heartwarming support and encouragement. In addition, I wish to appreciate Alev Keskin and Mustafa Demir for their precious help and assistance during this project .

Finally, I owe a great debt of gratitude to my family for always believing in me. I have been extremely fortunate to have this lovely family who has shown me unconditional love and spiritual support throughout my life. No words can express my gratitude to them.

This thesis is financially supported by The Scientific and Technological Research Council of Turkey (TÜBİTAK) under grant number 215E139 called "Doku Tanımlama Ve Gerçekleme İçin Dokunsal Sistem Tasarımı".

DECEMBER 2017 Farshad HAMEDI BAZZAZ

TABLE OF CONTENTS

Page

ABBREVIATIONS

DAQ : Data Acquisition
DC : Direct Current
DoF : Degree of Freedom
FEM : Finite Element Model
FFT : Fast Fourier Transform
MIS : Minimally Invasive Surgery
PVDF : Piezoelectric Polyvinylidene Fluoride
PZT : Lead zirconate titanate

SYMBOLS

$\mathbf{A}$	: Area of capacitance plate
$\mathbf{A_p}, \mathbf{A_s}$	: Surface area of piezoelectric/silicone layer
$\mathbf{A_{pi}}$	: Electrode's surface area at direction i
$\mathbf{b_p}, \mathbf{b_s}$	: Damping coefficient of piezoelectric/ silicone layer
$\mathbf{C}$	: Capacitance
$\mathbf{C_{10}}$,$\mathbf{C_{20}}$,$\mathbf{C_{30}}$	: Polynomial coefficients of the Yeoh model
$\mathbf{C_C}$, $\mathbf{C_{IN}}$	: Capacitance of connecting cables/ input amplifier circuit
$\mathbf{C_{FB}}$, $\mathbf{C_P}$	: Capacitance of feedback/ piezoelectric
$\mathbf{d}$	: Piezoelectric charge coefficients matrix
$\mathbf{d_c}$	: Distance between capacitance plates
$\mathbf{d_i}$	: Inter-taxel distance
$\mathbf{D}$	: Electric displacement or electric flux density vector
$\mathbf{e}$	: Piezoelectric strain coefficients matrix
$\mathbf{E}$	: Electric field vector
$\mathbf{E_s}$	: Elastic modulus of the silicone layer
$\mathbf{f}$	: Force
$\mathbf{g}$	: Piezoelectric voltage coefficients matrix
$\mathbf{h}$	: Piezoelectric pressure coefficients matrix
$\mathbf{I}$	: Current
$\mathbf{I_1}$	: Stress invariant
$\mathbf{k}$	: Silicone thickness layer
$\mathbf{k_p}, \mathbf{k_s}$	: Stiffness coefficient of piezoelectric/ silicone layer
$\mathbf{m_P}, \mathbf{m_S}$	: Mass of piezoelectric/ silicone layer
$\mathbf{P}$	: Macroscopic electric dipole
$\mathbf{P_{microscopic}}$	: Microscopic electric dipole
$\mathbf{Q}$	: Electrical charge
$\mathbf{Q_p}$	: Electrical charge of piezoelectric
$\mathbf{R}$	: Resistance
$\mathbf{R_C}$, $\mathbf{R_{IN}}$	: Resistance of connecting cables/ input amplifier circuit
$\mathbf{R_{FB}}$, $\mathbf{R_P}$	: Resistance of feedback/ piezoelectric
$\mathbf{s^E}$	: Elastic tensor measured at constant electric field
$\mathbf{S}$	: Strain tensor
$\mathbf{t}$	: Temperature
$\mathbf{t_p}, \mathbf{t_s}$	: Thickness of piezoelectric/ silicone layer
$\mathbf{T}$	: Stress tensor
$\mathbf{U}$	: Strain energy
$\mathbf{v}$	: Volume
$\mathbf{V}$	: Voltage
$\mathbf{V_{OUT}}$	: Voltage output of charge amplifier
$\mathbf{X_i}$	: Displacement amount of i^{th} mass
ε	: Permittivity constant

$\varepsilon^{\mathbf{S}}$: Dielectric permittivity tensor at constant strain
$\varepsilon^{\mathbf{T}}$: Dielectric permittivity tensor at constant stress
$\mu_{\mathbf{s}}$: Viscosity of the silicone layer

LIST OF TABLES

Page

LIST OF FIGURES

Page

MODELING AND DEVELOPMENT OF PIEZOELECTRIC BASED TACTILE SENSORS

SUMMARY

Humankind interacts with each other and their environment by their five senses: see, hear, touch, smell and taste. The touch sense has a significant role in humans daily life. This sense is responsible for perceiving force and its position, vibration, slip, temperature and pain. By development of robotic science, the need of interacting and collaborating between robots and humans has been increased. One of the ways to enhance the quality of this interaction between humans and robots is to produce touch sensitive robots and machines with the help of tactile sensors. Tactile sensors are the sensors with the ability of measuring and determination of physical properties such as pressure, vibration, softness, texture, shape and temperature through physical contact. Nowadays tactile sensors are used in a variety of applications in industry, robotic and healthcare fields. Tactile sensors are commonly used in automotive industry. The main purpose of utilizing tactile sensor in this industry is to measure the pressure distribution over a surface such as a seat or a brake pad to design more ergonomic components and increase the driving quality. Tactile sensors applications in the robotic field are mostly seen in robotic grippers. In these type of applications, the embedded tactile sensor is responsible to measure the applied force. With help of this sensor, the possibility of slippage or over forcing decreases. Besides all of these, tactile sensors have various applications in healthcare. Minimally Invasive Surgery (MIS) is one of the fields that using tactile sensor are getting popular. In this type of surgery, the tactile sensor is utilized in laparoscopic devices to avoid harming patient and help the surgeon to get information about the patient's body.

In this thesis, two types of human-inspired flexible tactile sensors have been proposed and their properties in term of sensitivity and flexibility have been compared. Even though the design of the proposed sensors is same, they are different in their sensing element. These sensing elements are Lead Zirconate Titanate (PZT) and Polyvinylidene Fluoride (PVDF) which are piezoceramic and piezopolymer types of piezoelectric respectively.

In the first chapter of this thesis, the aim of the project and the tasks defined for the sensors are explained. In literature review section, human touch mechanism, tactile sensors, and their application areas have been discussed. In the following the different sensing technologies used in the tactile sensors and their advantages and disadvantages have been described. Finally, piezoelectricity and piezoelectric constitutive relationships have been studied.

In the second chapter, the design parameters are defined. In order to study the effects of these parameters on the output voltage of the sensor, finite element model (FEM) of the single sensing unit (taxels) has been prepared. In the following, manufacturing steps of the proposed sensor have been described.

The third chapter theoretical model of single taxel and behavior of that to applied normal force has been investigated . In addition to state space model of taxels, transfer

function of charge amplifier used in measurements are obtained. Moreover, FEM modeling of the sensor and the silicone modeling has been explained briefly.
Finally, in the fourth chapter, the experimental setup and results are discussed. The response of piezoelectric taxels to impulse and step responses have experimented. Moreover, Frequency response function of the sensors has been obtained. Moreover, The effect of silicone thickness on taxel's output voltage is studied. Lastly, the force localization ability of the sensors tested and compared with each other.
In conclusion, it has been observed that both of the proposed tactile sensors are capable of force localization. However, PZT based tactile sensors are more successful in this task. In PVDF type tactile sensors crosstalk noises are seen commonly which decreases the quality of force localization. These human inspired tactile sensors with their compact designs can be embedded in robotic manipulators or they can be placed on the palm of the hand. It has been observed that the force sensitivity of PZT based tactile sensor is higher than PVDF one whereas the wearability of PVDF based tactile sensor is better due to the flexibility of PVDF materials.

DOKUNSAL PİEZOELEKTRİK ALGILAYICININ GELİŞTİRİLMESİ VE MODELLEMESİ

ÖZET

İnsanlık tarihinin başlangıcından beri, insanlar sahip olduğu beş algılama duyusunu kullanarak, birbirleriyle ve yaşadıkları çevreleriyle etkileşime geçerler. Algılamada görevli olan bu duyular; görme, işitme, dokunma, koklama ve tatma duyularıdır. Bu duyulardan biri olan dokunma duyusu, insanların günlük yaşantısında önemli bir role sahiptir. Dokunma; kuvvet ve konum algılamada, titreşim, sıcaklık ve acıyı hissetmede görevli bir duyudur. Robot biliminin gelişimiyle, robotlar ve insanlar arası etkileşme ve birbirleriyle iş birliğinde bulunma ihtiyacı ortaya çıkmıştır ve bu ihtiyaç gün geçtikçe artmıştır. Bu ihtiyacın karşılanması ve insanlar ile robotların etkileşimindeki kalitenin iyileştirilmesi için geliştirilen yollardan biri ise dokunsal algılayıcılar yardımıyla, dokunmaya duyarlı robotlar ve makinalar üretilmesidir. Dokunsal algılayıcılar; fiziksel temas yoluyla oluşan basınç, titreşim, yumuşaklık, doku, şekil ve sıcaklık gibi fiziksel özellikleri ölçebilen ve tayin edebilen algılayıcılardır.

Günümüzde, dokunsal algılayıcıların endüstri, robotik ve sağlık hizmetleri gibi alanlarda çok çeşitli uygulamaları vardır. Bu algılayıcılar yaygın olarak otomotiv sektöründe kullanılırlar. Otomotiv sektöründe kullanılan dokunsal algılayıcıların en öncelikli amacı, daha ergonomik parçalar tasarlamak ve sürüş kalitesini arttırmak için bir yüzey boyunca basınç dağılımını ölçmektir. Örneğin; bir koltuk veya diskli fren balatası gibi yüzeylerde kullanılırlar. Robotik alanındaki dokunsal algılayıcılar ise, çoğunlukla robot el uygulamalarında görülür. Bu tarz uygulamalarda kullanılan gömülü dokunsal algılayıcılar, robot parmaklarına uygulanan kuvveti ölçmek ile yükümlüdürler. Böylece, parmaklar arasında meydana gelen kayma veya aşırı kuvvet uygulanma olasılığı bu algılayıcıların yardımıyla en aza indirgenir. Bütün bunların yanında, dokunsal algılayıcıların sağlık alanında da çok çeşitli uygulamaları vardır. Minimal İnvaziv Cerrahi (Laparoskopik Cerrahi) dokunsal algılayıcıların popüler olduğu uygulama alanlarından bir tanesidir. Bu tarz ameliyatlarda, laparoskopik cihazların hastaya zarar vermesini engellemek ve cerrahın, hastanın bedeni hakkında bilgi almasına sağlamak amacıyla dokunsal algılayıcılardan yararlanılır.

Günümüzde, dokunsal algılamada kullanılan birçok algılama teknolojisi vardır. Bu teknolojilerden bazıları, kapasitif, piezoresistif, optik ve piezoelektrik esaslı çalışan algılayıcılardır. Kapasitif esaslı dokunsal algılayıcılarda yüksek duyarlılık, statik kuvvet ölçüm kabiliyeti ve kabul edilebilir frekans yanıtı olmasına rağmen, bu tarz algılayıcılarda çapraz karışma gürültüsü veya alan etkişleşimleri gibi sorunlar meydana gelebilir. Piezoresistif dokunsal algılayıcılar ise basit yapıda olması ve yüksek algılama aralığına sahip olması nedeniyle tercih edilmektedirler. Ancak, bu algılayıcılarında bazı dezavatajları vardır. Bunlar, histerezis ve düşük frekans yanıtına sahip olmalarıdır. Optik esaslı dokunsal algılayıcılar, geniş ölçüm aralığına ve yüksek tekrarlanabilirliğe sahiptirler. Bu algılayıcıların başlıca dezavantajları boyutları ve sertlikleridir. Bu dezavantajlar yüzünden giyilebilir ve gömülebilir değillerdir. Bu

proje kapsamında, piezoelektrik malzemeler kullanılmıştır. Bu malzemeler, dinamik yanıtlarının iyi olması ve zaman yanıtlarının hızlı olması nedeniyle tercih edilmiştir. Ayrıca, bu malzemelerin endüklenmiş elektrik yükü ile uygulanan mekanik kuvvet arasındaki ilişkinin lineer olması tercih edilmesinde rol oynamıştır.

Bu tezde, insandan ilham alınarak gerçeklenmiş esnek iki tip dokunsal algılayıcı önerilmiştir. Aynı zamanda, bu iki algılayıcının hassaslık ve esneklik bakımından özellikleri karşılaştırılmıştır. Önerilen algılayıcıların tasarımları aynı olmasına rağmen, algılama elemanları bakımından birbirinden farklılardır. Bu algılama elemanları, Kurşun Zirkonat Titanat (Lead Zirconate Titanate-PZT) ve Polivinilidin Florür (Polyvinylidene Fluoride - PVDF) bileşenli olan ve sırasıyla piezoseramik ve piezopolimer olarak bilinen piezoelektriğin türlerindendir.

Bu tezin ilk bölümünde, projenin amacı ve algılayıcılar için tanımlanmış görevler açıklanmıştır. Kuvvet lokalizasyonu,şekil tanıma ve sertlik algılama önerilen algılayıcıların görevlerinden birkaçıdır. Literatür incelemesi bölümünde ise, insan dokunma mekanizması, dokunsal algılayıcılar ve bunların uygulama alanları tartışılmıştır. Bunlara ilaveten, dokunsal algılayıcılarda kullanılan farklı algılayıcı teknolojileri, avantajları ve dezavantajları tanımlanmıştır. Son olarak, piezoelektrik etki ve piezoelektrik yapısal bağlantıları incelenmiştir.

Tezin ikinci bölümünde, silikon kalınlığı ve iki dokunma biriminin arasındaki mesafe tasarım parametreleri olarak tanımlanmıştır. Bu parametrelerin algılayıcının çıkış voltajı üzerindeki etkisinin incelenmesi amacıyla, tekli dokunma biriminin sonlu elemanlar modeli (Finite Element Model-FEM) oluşturulmuştur. Devamı olarak, önerilen algılayıcının üretim aşamaları açıklanmıştır.

Projede geliştirilen dokunsal algılayıcılar çoklu katmanlı yapıya sahiptirler ve katman katman üretimi yapılmıştır. Bu katmanların ikisi elektrot katmanı (bir tanesi ortak toprak elektrotu), biri algılama elemanı ve diğer iki katman ise silikon kaplamalıdır. Algılayacı dizaynında silikon kaplama kullanılmasının sebebleri, algılayacıları darbelere karşı daha dayanıklı yapmak, daha kompakt bir yapıya sahip olmasını ve giyilebilir olmasını sağlamaktır. Özellikle PZT tipli piezoelektrik algılayacılarda, algılama elemanının kırılgan olması sebebinden dolayı, silikon kaplamanın önemi daha fazladır. Bu kaplama tabakası algılayacı üzerinde uygulanabilir kuvvet aralık miktarını arttırır ve PZT'yi kırılmaktan korur.

Tezin üçüncü bölümünde, tekli dokunma biriminin kuramsal modeli ve uygulanan normal kuvvetteki davranışı incelenmiştir. Dokunma biriminin durum uzay modeline ek olarak algılayıcı ölçümlerinde kullanılan yük kuvvetlendiricisinin transfer fonksiyonu elde edilmiştir. Bunların yanısıra, algılayıcının ve silikonun sonlu elemanlar kullanılarak (FEM) modellemesi kısaca açıklanmıştır.

Son olarak tezin dördüncü bölümünde, deney düzeneği anlatılmış ve deney sonuçları tartışılmıştır. Piezoelektrik dokunma birimlerinin impuls ve basamak yanıtlarına cevapları gözlemlenmiştir. PZT ve PVDF esaslı algılayıcıların ikisi de kuvvet girdisine göre birinci dereceden sistem davranışı göstermişlerdir ve bu davranış bilgisiyle sistemlerin zaman sabitleri de hesaplanmıştır.Algılayıcı elemanlar aynı tipte olmalarına rağmen, elde edilen zaman sabitleri birbirinden farklıdır. Bu bölümde elde edilen zaman sabitleri daha sonra algılayıcı elemanlarının kalibrasyonunda kullanılmışlardır. Buna ek olarak, dokunsal algılayıcı üzerindeki uygulanan kuvvet ve çıkış voltajı arasındaki ilişki incelenmiştir. Bu incelemeler sonucunda beklenildiği gibi ilişkinin lineer olduğu gözlemlenmiştir. PZT ve PVDF esaslı dokunsal algılayıcıların korelasyon katsayıları sırasıyla 0,9942 ve 0,9933 olarak hesaplanmıştır. Çalışmanın devamında, algılayıcıların frekansa bağlı fonksiyonu elde edilmiştir. Ayrıca, silikonun

kalınlığının dokunma birimlerinin çıkış voltajları üzerindeki etkisi incelenmiştir. Daha sonra algılayıcıların kuvvet lokalizasyon becerisi test edilmiş ve bu beceriler birbirleriyle karşılaştırılmıştır. Bu bölümün en son kısmında ise, yapılan deneylerden elde edilen sonuçlar ile üçüncü bölümde hesaplanan tekli dokunma biriminin kuramsal ve sonlu elemanlar modeli frekans yanıtı açısından karşılaştırılmıştır. Bu karşılaştırmalar sonucunda karakök ortalama yöntemiyle bulunan hata oranları hesaplanmıştır. Tekli dokunma biriminin kuramsal modeli için bulunan hata oranı %9,75 ve sonlu elemanlar modeli için bulunan hata oranı ise %11,58'dir.

Sonuç olarak, önerilen dokunsal algılayıcıların ikisinin de kuvvet lokalizasyonu yapılabildiği gözlemlenmiştir. Ancak, PZT esaslı dokunsal algılayıcıların bu görevde daha çok başarılı olduğu ortaya çıkmıştır. PVDF esaslı dokunsal algılayıcılarda genellikle kuvvet lokalizasyon kalitesini azaltan çapraz karışma (crosstalk) gürültüleri görülmüştür. İnsandan ilham alınarak yapılan ve kompakt tasarımlara sahip olan bu dokunsal algılayıcılar, robotik manipülatörlere entegre edilebilir veya insanın avuç içine yerleştirilebilirler. PZT esaslı dokunsal algılayıcıların kuvvet duyarlılığı, PVDF esaslı olanlara göre daha fazlayken, PVDF esaslı dokunsal algılayıcıların giyilebilirliği, PVDF malzemelerin esnekliğinden dolayı daha iyidir.

1. INTRODUCTION

1.1 Aim of The Project

Sensors with the ability of measuring and determination of physical properties such as temperature, vibration, softness, texture, shape, composition and forces through physical contact are named as tactile sensors [8]. These sensors are widely used in industry, robotic and healthcare fields. For example, tactile sensors are used in automotive industry to measure and visualize dynamic pressure distribution between driver and car seat during actual driving and braking is one of the applications of tactile sensing in automotive industry. With help of this measurement, car seat manufactures can develop more comfortable seat which applies less force to driver and increases the quality of driving [9]. In the robotic area, tactile sensors are widely utilized in robot manipulators to acquire information during grab, hold and handle functions. With the help of the tactile sensor, the probability of harming objects due to over force application or slippage can be decreased [10]. Nowadays with the development of robotic science, the usage of Minimal Invasive Surgery (MIS) has been increased. Less recovery time and negative impact on patient are the main advantages of this type of surgery. Detection of tumors presented in soft tissues is one of the illustrations of usage of tactile sensor in MIS and healthcare. [11] The aim of the project is to propose flexible and wearable tactile sensors that is inspired from human skin. We have used two different sensing element which is called as "taxels" representing receptors in human tissue. In this thesis we compared the properties of the taxels in terms of their signal robustness and sensitivity. The sensing material of materials have been chosen as PZT and PVDF which are two different types of piezoelectric materials. The reason of utilizing piezoelectric material is the high sensitivity, fast response time of these materials. Moreover, Human skin with help of tactile mechano-receptors can sense vibrations till 300 Hz [12]. Therefore, piezoelectric based sensing mechanism which has high dynamic response is a suitable choice for this design criteria.

PZT is the most common used piezoceramic with high piezoelectricy property whereas PVDF is the most popular type of piezo polymer material. Force measuring and localization, stiffness measuring, roughness and texture estimations are the tasks defined for this sensor whilst the wearability and flexibility of the sensors are always considered during design. These novel sensors propose compact design, flexibility and high repeatability. It can be embedded in robotic systems such a robotic grippers/hands to measure applied force on the specimen in order to avoid slippage or harming the specimen. It can be worn by medical devices/probes for diagnostics because it can detect different kinds or stiffness which can be used to distinguish tumors.

1.2 Literature Review

In this section, human touch sense and tactile sensing will be explained briefly. In the following, application areas of the tactile sensors and the most common used sensing technologies in tactile sensing will be described. Moreover, advantages and disadvantages of these technologies will be discussed. Finally, piezoelectricity and piezoelectric constitutive relationships will be explained.

1.2.1 Human touch sense and tactile sensing

Human interact with their environment by using their five senses: see, touch, smell, hear and taste. In human body, the touch sense is responsible of perceiving force, force position, vibration, slip, temperature and pain [13]. Skin with surface are of nearly 1.6 m^2 is the largest sensory organ on human. In addition to sensing function, skin have other responsibilities such as: protecting body from bacteria, thermal control, secretion, excretion, synthesis of vitamins, and breathing [14]. There are four kinds of tactile receptor (mechanoreceptors) in human skin which are distributed all over the body (Figure 1.1). These four mechanoreceptors are: the Meissner corpuscles, the Merkel cells, the Ruffini endings, and the Pacinian corpuscles. Meissner corpuscles mechanoreceptors are in charge of sensitivity to light touch. These receptors are distributed throughout the skin and they are mostly concentrated in areas sensitive to light touch such as fingertips or lips. Markel cells are other types of mechanoreceptors found in the top layer of the skin which are known as the most sensitive mechanoreceptor to low frequency vibrations. Ruffini

endings mechanoreceptors are sensitive to skin stretch. These receptors contribute to the kinaesthetic sense and control of position and movement of fingers. Finally, Pacinian corpuscles which are placed in deep subcutaneous tissue, are responsible of sensing high frequency vibration. Unlike Ruffini endings and Markel cells, Pacinian corpuscles Are rapidly adapting receptors. They just respond to rapid indentation of skin and they cannot sense steady pressure. [15]

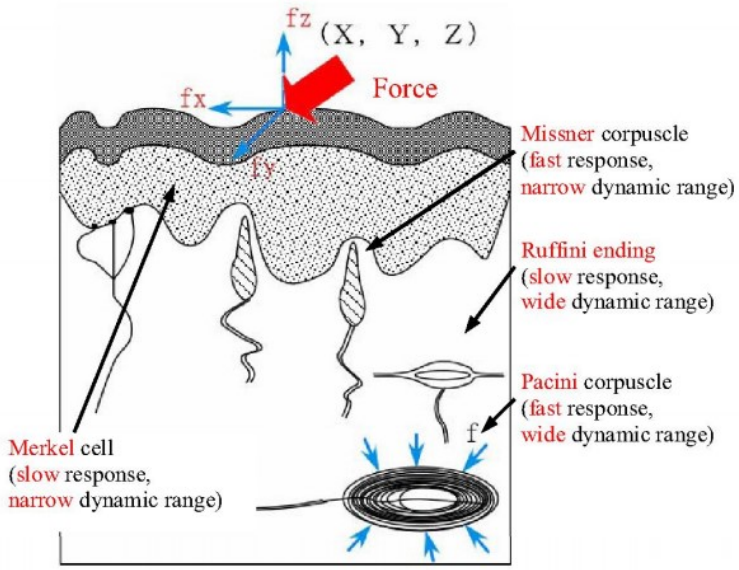

Figure 1.1 : Tactile receptors of human skin [1]

Sensors which can determine properties such as temperature, vibration, softness, texture, shape, composition and shear or normal forces by physical contact are categorized as tactile sensors [8]. With development of robotic science, robots are having more significant role in human's lives and interaction between human and robots have been increased. tactile sensing of the machines is one of the ways to increase the quality of this interaction. For the first time, in the 1980s Harmon predicted the ability of tactile sensing to be integrated into robotics field [16] [17] [18]. The design criteria that he proposed are frequently used by researchers to justify their research direction. [19]. In 21st century the main research topics and motivations is about the developing sensors to be used in biomedical areas and unstructured environments whereas in the 1970 and 1980s the main idea was about to develop sensing system for intelligent robotics.

Nowadays, the main applications of tactile sensors can be classified in three cases: Industrial, Robotic and healthcare. Automotive industry is one of the industries which

commercially tactile sensors are used. In this industry tactile sensors contribute to test and monitor pressure distribution and redesign in order to increase quality of driving and safety. Monitoring dynamic pressure distribution in hinges and door latches, brake pedal and seat are examples of tactile sensing usage in automotive industry (Figure 1.2).

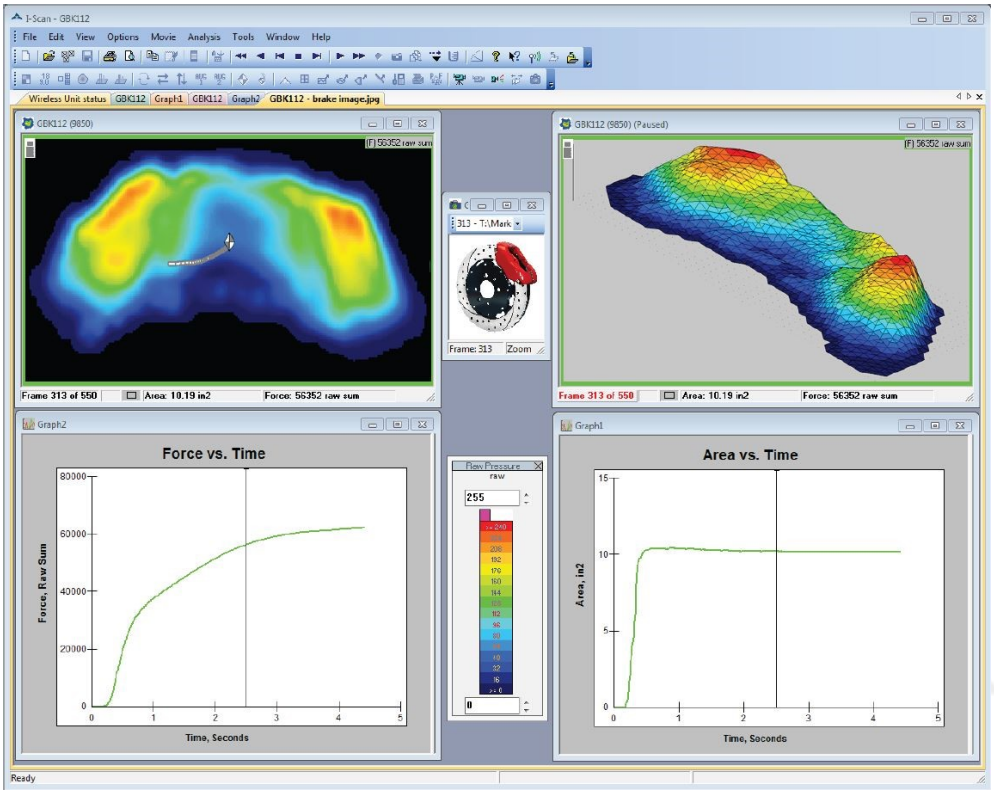

Figure 1.2 : Example of usage of tactile sensor in automotive area: Pressure distribution between a brake pad and rotor [2]

Another field that can be got advantage of tactile sensing is the robotic field. The importance of tactile sensors in robot manipulators are significant. These sensors can help to the manipulators in handle, grab and hold object to avoid slippage and over force application. Object and texture recognition and measuring stiffness, force and temperature are the examples of the needs which can be met by help of tactile sensing [20] (Figure 1.3).

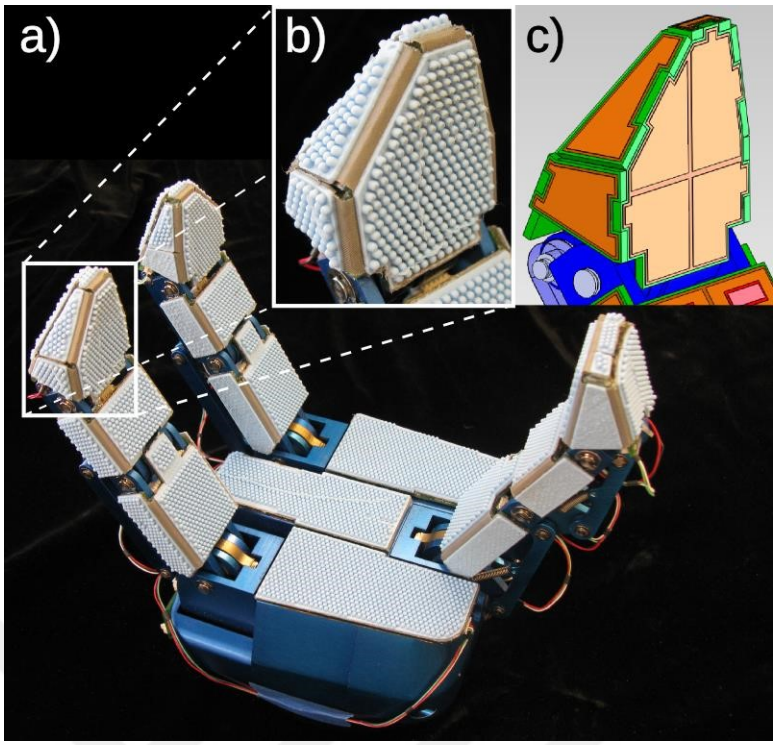

Figure 1.3 : Example of usage of tactile sensor in robotic area: Adaptive gripper with sensor suite installed (a). Closeups show (b) texture and (c) taxels [3].

Tactile sensors can have significant role in healthcare. By developing in robotic technology, the number of minimally invasive surgeries (MIS) have been increased. The reason why MIS is preferred is because of less recovery time, hospital stay and post-surgery side effects. In MIS, a laparoscopic device is carried out through the skin, body cavity or anatomical opening and with the help of that, remote control manipulation of instrument and indirect observation can be done [15]. These laparoscopic devices can be equipped by tactile sensors to distinguish tumor from soft tissue [11]. In addition to that, tactile sensors can be utilized as an alternative to ultrasound based systems and mammography in order to detect cancer [21] (Figure 1.4).

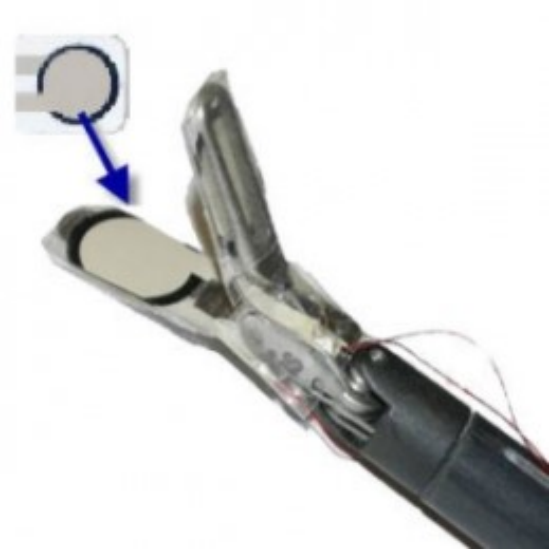

Figure 1.4 : Example of usage of tactile sensor in healthcare area:Tactile Feedback Robotic Surgery [4].

1.2.2 Sensing mechanism of tactile sensors

Tactile sensors convert the measured physical properties (such as force, heat, etc.) to electrical signals. These sensors can be classified according to their sensing mechanism to capacitive, piezoresistive, piezoelectric and optical based tactile sensors.

1.2.2.1 Capacitive based tactile sensors

Capacitive based sensors are consisting of dielectric material which is placed between two plates of conductive plates. The capacitance 'C' can be denoted by

$$C = \varepsilon \frac{A}{d_c} \tag{1.1}$$

In equation 1.1, 'A' represents the area of the capacitance plate and 'd_c' denotes the distance between two conductive plates and 'ε' is the permittivity constant. When a capacitive based tactile sensor is subjected to force, the distance between two conducting plates changes and this lead to change in capacitance value of the capacitance. With the help of this capacitance change, normal force [46], shear forces [47] and strains [47] can be measured [22] [23] [24]. High sensitivity, static force measurement, compatibility, acceptable frequency response, high spatial resolution and large dynamic range are the advantages of the capacitance based tactile sensor.

Despite of these advantages, these sensors due to crosstalk noise, field interactions and fringing capacitance are susceptible to noise. In order to filter out the produced noise, relatively complex electronics are needed.

1.2.2.2 Piezoresistive based tactile sensors

The principle of piezoresistive tactile sensor is based on change of electrical resistance in a material upon application of force. The relation between voltage 'V', current 'I' and resistance 'R' of a simple resistance can be expressed by:

$$V = IR \tag{1.2}$$

In these types of the sensor since the resistance value is variable, either voltage or current will be fixed and by measuring the change in the other parameter, the force is estimated [25] [26].Conductive rubber, elastomer, or conductive ink are the typical resistive elements used in tactile sensors. Hysteresis and low frequency response (in comparison to capacitive and piezoelectric tactile sensors) are the main drawbacks of these sensors. However, piezoresistive tactile sensors are preferred owing to their structure simplicity, low energy consumption and high detection range. In addition, piezoresistive materials are less noise sensitive and in case of mesh configuration, there is no cross talk or field interaction.

1.2.2.3 Optical based tactile sensor

These sensors measure physical properties such as strain or surface texture by help of physical properties like light intensity. These sensors which mostly are composed of light source, optical detector and optical waveguide are not sensitive to electromagnetic interface. Besides, high resolution, wide measurement range and high repeatability are other benefits of this sensing mechanism. The main downside of the optical based tactile sensors are their size and rigidness which causes inability of embedment and poor wearability of these sensors [27] [28].

1.2.2.4 Piezoelectric based tactile sensor

Some certain crystalline materials generate electrical charge proportional to the applied mechanical stress. This property of these crystalline materials are called piezoelectricity [29]. The materials which exhibit piezoelectricity are called

piezoelectric. Owing to high frequency response, these materials are widely used for measurement of vibration, sound, slip and surface roughness discrimination [30] [31] [32]. In addition to these, high sensitivity, fast response time and low power-consumption are the reasons of selecting piezoelectric materials as sensing mechanism of tactile sensors. However, the charge induced in piezoelectric materials are temperature dependent which can be considered as a drawback for these materials. Another disadvantage of these material is inability to measure static forces. In the case of applying static force no charge will be induced in piezoelectric materials.

1.3 Piezoelectricity

In this project, after investigating technologies used in tactile sensing, piezoelectric materials are selected as the sensing element. Fast response, high sensitivity and good dynamic response are the reasons of utilizing these materials in the proposed tactile sensor. In the following sections history, structure and constitutive relationships of piezoelectric material are discussed.

1.3.1 History

In 1880 Curie brothers discovered that specially prepared crystals (like: tourmaline, quartz, topaz, cane sugar and Rochelle salt among them), develop surface electrical charges under mechanical pressure. This phenomenon was named “Piezoeffect” and the materials such as quartz, turmalin and segnet which show this behavior were called “Piezoelectric”. Moreover, the electricity generated by mechanical stress was called “Piezoelectricity”. [33]The word “Piezo” is derived from Greek word for pressure.
In 1881, G. Lippmann predicted that mechanical pressure and elastic deformation would be caused by applying electric field on piezoelectric materials [34]. This property which was mathematically deduced from fundamental thermodynamic principles was confirmed by Cuires and named as “converse piezoelectric effect” [35]. For the next few decades, due to the complexity of piezoelectricity science, piezoelectric materials were not used in practical application. During these years, moststudies were about the relation between crystal structures and piezoelectricity. This studies led to the publication of Lehrbuch der Kristallphysik (a textbook on crystal

physics). In this book, Woldemar Voigt explained the 20 natural crystal types which exhibit piezoelectricity and stated piezoelectric constant by tensor analysis [36] [37]. The first practical use of piezoelectric material suggested by Paul Langevin in 1917. In order to detect underwater objects, he developed an ultrasonic echo ranging device which resulted in modern echo sounders and underwater detection devices [38] [39].

As it mentioned before, piezoelectricity has two direct and converse effects and nowadays these materials are used in automotive, computer, medical and military fields. In sensor and voltage generating technologies,the direct piezoelectric effect of piezoelectric materials is utilized. Force, pressure and accelerometer sensors are examples of piezoelectric sensors. Also, these materials can be used as voltage generators in spark ignitors. The applications for the converse effect of piezoelectrics ultrasonic generators, oscillators, piezoelectric motors and nano/micro positioning are the example of devices which their working principle is based on converse piezoelectric effect.

1.3.2 Crystallographic structure of piezoelectric materials

Piezoelectric materials can be found in two forms of ceramic and polymer. Barium titanate and lead zicronate titanate are examples of piezoceramics whereas polyvinylidene difluoride is the most popular type of piezo polymer.

Most of piezoceramics have $A^{2+}B^{4+}O_3^{2-}$ general formulation. In this notation, 'A' represents large divalent metals like lead or barium. 'B' denotes metal ions such as zirconium and titanium which have tetravalent structure. Finally, 'O' stands for oxygen. These types of materials according to their temperature, show different crystal structures (Figure 1.5) [6]. In the temperature below the Curie temperature (which is usually 300°C- 400°C), the crystal structure of these piezoelectrics are tetragonal shaped. Since the position of B^{4+} ion is not symmetric, a microscopic electric dipole is created within the unit cell. Even though there is an electric dipole in microscale, the resultant macroscopic electric dipole is zero.

$$P = lim_{\Delta v \to 0} \frac{\sum_{\Delta v} P_{microscopic}}{\Delta v} \tag{1.3}$$

However, In the temperature above Curie temperature, the crystal shape change into cubic structure. In this structure, due to position of B^{4+} in the middle of lattice and the coincidence of positive and negative charges, the net dipole moment is equal to zero.

As a result, the macroscopic dipole of the material will be equal to zero.

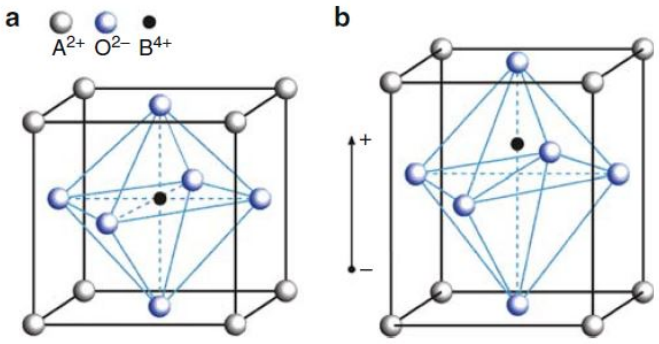

Figure 1.5 : Piezoceramics cell Crystallographic structure, (a) cubic lattice above Curie temperature, and (b) tetragonal lattice below Curie temperature [5]

There is a tendency of dipoles to have local regions and alignment inside the material which is called Weiss Domain. Due to random arrangement of Weiss domains and their different dipole moments, the net polarization of material will be zero. In order to align these Weiss domains and create polarization within the material, the specimen is immersed in 100-150°C transformer oil whilst it is subjected to a static electric field of 2.5-4.5 MV/m for 10-20 minutes. With help of this process, the local dipoles will be placed in the direction of applied electric field. After removing the electric field, the most of dipoles, remain at their position (Figure 1.6). This phenomenon which is called remanent polarization, makes the ceramic permanently piezoelectric.

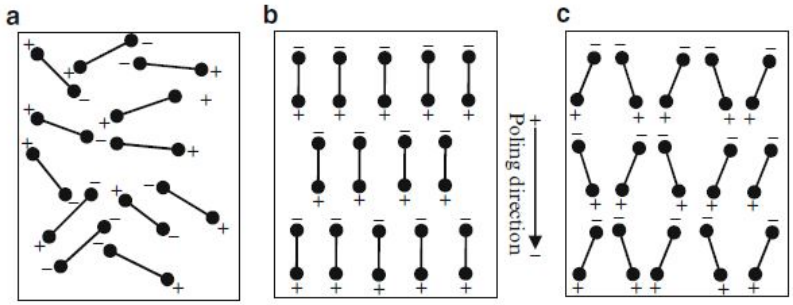

Figure 1.6 : Schematic representation of electric dipoles in Weiss domains: (a) before polarization, (b) during polarization, and (c) after polarization [6]

1.3.3 Piezoelectric constitutive relationships

According to IEEE for the unbounded piezoelectric medium, the constitutive relation can be written as [40]:

$$S_{ij} = s^{E}_{ijk} T_{kl} + \left[d_{ijk}\right]^{T} E_k \tag{1.4}$$

$$D_i = d^{T}_{ijk} T_{kl} + \varepsilon^{T}_{ik} E_k \tag{1.5}$$

Where:

- S_{ij}: strain tensor coefficient (second-rank)
- s^{E}_{ijkl}: elastic coefficient measured at constant electric field (fourth-rank tensors)
- T_{kl}: stress tensor coefficient (second-rank)
- d_{kij}: piezoelectric coefficient (third-rank tensor)
- E_k: electric field coefficients (firth-rank tensor)
- D_i: Electric displacement or electric flux density coefficient (firth-rank tensor)
- ε^{T}_{ik}: dielectric permittivity at constant stress (second-rank tensor)

The element number of above tensors are dependent to the rank of them. For example, third-rank and fourth-rank tensors have 27 and 81 elements respectively. Due to transversely isotropic properties of piezoelectrics [41] and crystal symmetry properties, by defining suitable reference axes and planes, previously discussed tensors can be simplified. Therefore, direction 3 is set as poling direction, 1 as length and 2 as width of the piezoelectric. Planes 4,5 and 6 are planes orthogonal to axes 1,2 and 3 respectively and represent shear planes (Figure 1.7).

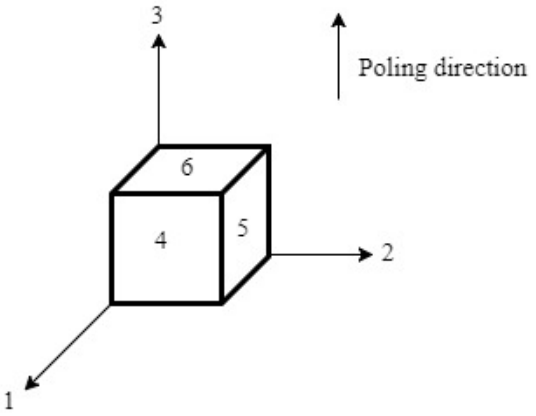

Figure 1.7 : Schematic representation of planes and directions

With this representation, stress, strain and electric displacement tensors are simplified as 6x1 vectors. Moreover, electric field, piezoelectric coefficients, dielectric permittivity and elastic coefficient tensors can be written as 3x1, 6x3, 3x3 and 6x6 matrices respectively. So the final formula can be written as [42]:

$$S = s^E T + \left[d\right]^T E \tag{1.6}$$

which can be written as:

$$\begin{bmatrix} S_1 \\ S_2 \\ S_3 \\ S_4 \\ S_5 \\ S_6 \end{bmatrix} = \begin{bmatrix} s_{11} & s_{12} & s_{13} & 0 & 0 & 0 \\ s_{12} & s_{22} & s_{23} & 0 & 0 & 0 \\ s_{13} & s_{23} & s_{33} & 0 & 0 & 0 \\ 0 & 0 & 0 & s_{44} & 0 & 0 \\ 0 & 0 & 0 & 0 & s_{55} & 0 \\ 0 & 0 & 0 & 0 & 0 & s_{66} \end{bmatrix} \begin{bmatrix} T_1 \\ T_2 \\ T_3 \\ T_4 \\ T_5 \\ T_6 \end{bmatrix} + \begin{bmatrix} 0 & 0 & d_{31} \\ 0 & 0 & d_{32} \\ 0 & 0 & d_{33} \\ 0 & d_{24} & 0 \\ d_{24} & 0 & 0 \end{bmatrix} \begin{bmatrix} E_1 \\ E_2 \\ E_3 \end{bmatrix} \tag{1.7}$$

also,

$$D = dT + \varepsilon^T E \tag{1.8}$$

$$\begin{bmatrix} D_1 \\ D_2 \\ D_3 \end{bmatrix} = \begin{bmatrix} 0 & 0 & 0 & 0 & d_{15} & 0 \\ 0 & 0 & 0 & d_{24} & 0 & 0 \\ d_{31} & d_{32} & d_{33} & 0 & 0 & 0 \end{bmatrix} \begin{bmatrix} T_1 \\ T_2 \\ T_3 \\ T_4 \\ T_5 \\ T_6 \end{bmatrix} + \begin{bmatrix} \varepsilon_{11} & 0 & 0 \\ 0 & \varepsilon_{22} & 0 \\ 0 & 0 & \varepsilon_{33} \end{bmatrix} \begin{bmatrix} E_1 \\ E_2 \\ E_3 \end{bmatrix} \tag{1.9}$$

As it mentioned before, since piezoelectric material is inversely isotropic in the plane 3, the following equalities are valid: $s_{11} = s_{22}, s_{13} = s_{23}, s_{44} = s_{55}$. By integrating Electric displacement over the electrode surfaces, the accumulated electric charge can be calculated [43]:

$$q = \iint \begin{bmatrix} D_1 & D_2 & D_3 \end{bmatrix} \begin{bmatrix} dA_{p1} \\ dA_{p2} \\ dA_{p3} \end{bmatrix} \tag{1.10}$$

1.3.4 Piezoelectric parameters

The signal generating and mechanical actuating behavior of piezoelectric materials can be estimated by parameters such as: dielectric permittivity and piezoelectric charge constant. Some of these parameters like permittivity, are influenced by stress and electric field. Superscript T and E is the property measured at constant stress and electric field respectively.

Dielectric Permittivity ε: It is seen that voltage generated by piezoelectric material 'V' is dependent to induced charge 'Q' inversely related by capacitance 'C'.

$$Q = CV \tag{1.11}$$

One of the most important factors in capacitance, is dielectric permittivity. By increasing permittivity of the piezoelectric, the capacitance value of the material is increased and as a result, output voltage is lowered. The relation of parallel plate capacitor is given below:

$$C = \varepsilon \frac{A}{d_c} \tag{1.12}$$

In equation 1.12 'A' represent area and and 'd_c' denotes the distance between two conductive plates. Permittivity is measured in constant stress (with super script T) and constant strain (with superscript S). The relation between these two dielectric permittivity matrices can be expressed as functions of $\left[e\right]^T$ and d which are transpose of piezoelectric strain matrix and piezoelectric charge constant respectively :

$$\varepsilon^S = \varepsilon^T - \left[e\right]^T d \tag{1.13}$$

Piezoelectric charge matrix 'd', can be defined in two manners.The first definition is the amount of electric displacement developed for the applied stress. In this definition, the unit of 'd' is Columbus per Newton (C/N). 'd' matrix is composed of 'd_{ij}' elements (equation 1.14).

$$d = \begin{bmatrix} 0 & 0 & 0 & 0 & d_{15} & 0 \\ 0 & 0 & 0 & d_{24} & 0 & 0 \\ d_{31} & d_{32} & d_{33} & 0 & 0 & 0 \end{bmatrix} \tag{1.14}$$

The first subscript of 'd', indicates the direction of induced electric displacement and the second one represents the direction of mechanical stress. For example, 'd_{33}'

represents the coefficients when both electric displacement and mechanical stress are in the same direction along polarization of the piezoelectric.

It should be noted that due to planar isotropy properties d_{32}=$d_{31}$and d_{24}=d_{15}. The second definition of d is useful for actuator usage of piezoelectric. It shows the relation between strain induced in piezoelectric for the applied electric field unit. According to this definition, the first and second subscripts show the strain and applied electric field unit direction respectively. The above definitions can be summarized in equation 1.15 [44].

$$d = \left(\frac{\partial s}{\partial E}\right)_{T,t} = \left(\frac{\partial D}{\partial T}\right)_{E,t} \tag{1.15}$$

Piezoelectric voltage matrix g: In sensor and generator application of piezoelectrics, voltage constant is significant criteria that should be considered during design. Similar to piezoelectric charge constant, voltage constant 'g' can be describe piezoelectric properties in two ways. g can be defined as the amount of electric field produced while mechanical stress is applied (unit: $V.m/N$). At the same time, it can be expressed as ratio of strain induced for electric displacement (m^2/C) [45].

$$g = -\left(\frac{\partial E}{\partial s}\right)_{D,t} = \left(\frac{\partial s}{\partial D}\right)_{T,t} \tag{1.16}$$

The relation between d and g constant can be written like below:

$$d/g = \frac{\left(\frac{\partial s}{\partial E}\right)_{T,t}}{\left(\frac{\partial s}{\partial D}\right)_{T,t}} = \left(\frac{\partial D}{\partial E}\right)_{T,t} = \varepsilon^T \tag{1.17}$$

i.e.:

$$\frac{d_{ij}}{g_{ij}} = \varepsilon_{ii}^T \tag{1.18}$$

Whereas ε^T is permittivity of piezoelectric in constant stress.

Piezoelectric strain coefficients matrix e: Another useful piezoelectric constant used in calculations is piezoelectric strain constant. This constant is used in alternative forms of piezoelectric constitutive relationships. Definition of 'e' can be expressed as :

$$e = \left(\frac{\partial D}{\partial s}\right)_{E,t} = -\left(\frac{\partial T}{\partial E}\right)_{S,t} \tag{1.19}$$

'e' coefficient is the amount of electric displacement produced per strain in constant electric field. Moreover, this constant represents the amount of stress produced when the piezoelectric is subjected to electric field at constant strain.

Piezoelectric pressure coefficients matrix h: this matrix shows the electric field generated for the applied strain while electric displacement remains constant. According to converse piezoelectric effect it is the ratio of measured stress to applied electric displacement at constant strain.

$$-h = \left(\frac{\partial E}{\partial s}\right)_{D,t} = \left(\frac{\partial T}{\partial D}\right)_{S,t} \tag{1.20}$$

2. DESIGN AND MANUFACTURING

The presented human inspired tactile sensors (Figure 2.1 and 2.2), are designed to be wearable on the palm of a hand or arm. Moreover, it can also be mounted or on a robotic gripper. So, the suggested sensors have to be small, soft, flexible and wearable by considering manufacturing limits such as 3d printer and laser cutting machine precision. As it mentioned in section 1.2.1, there are four types of mechanoreceptor in human skin which are responsible of touch sense (Figure 1.1). With help of these touch receptors, Shape, edge and textures of objects can be recognized and the pressure and its location can be sensed by human.

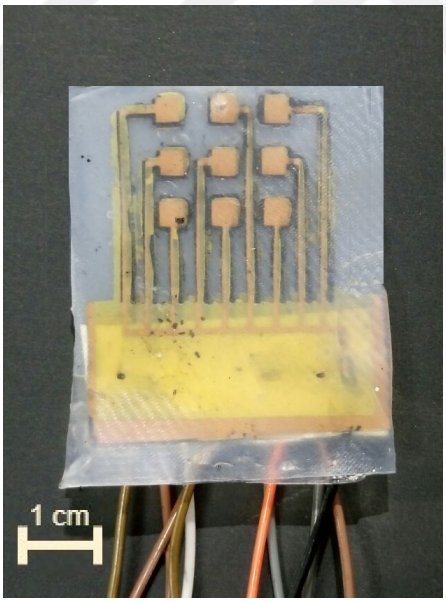

Figure 2.1 : Picture of the proposed silicone embedded PZT based tactile sensor.

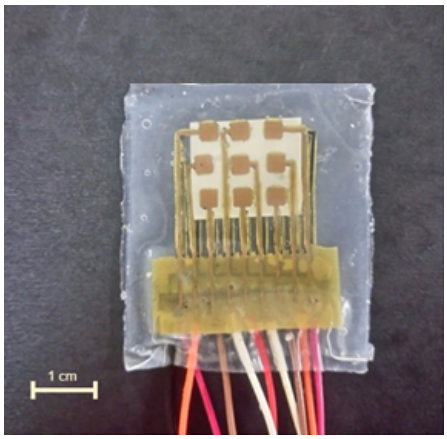

Figure 2.2 : Picture of the proposed silicone embedded PVDF based tactile sensor.

Human skin is the inspiration source of this project. Designing a tactile sensor with ability of force measuring, localization and capable of texture and shape recognition was the goal of this project. In order to fulfill these needs, two sensors comprised of 3x3 matrix taxels embedded in silicone (Ecoflex 30; smooth-on) are developed (Figure 2.3). Taxel is the unit of tactile sensing element and likewise mechanoreceptors in human skin, they are responsible of touch sensing in tactile sensors. In this study two types of sensing elements are utilized: Lead zirconate titanate (PZT) and Polyvinylidene fluoride (PVDF). These sensing elements distinct in piezoelectricity and elasticity properties which lead to diversified behavior of the sensors in produced electrical charge and mechanical properties like flexibility (Table 2.1) [46].

Table 2.1 : PZT and PVDF properties.

Property	PSI 5H-4E [47]	PVDF [48]
Density (Kg/m^3)	7800	1780
Thickness (mm)	0.127	0.052
d_{33} $(Coulomb/Newton)$	650×10^{-12}	23×10^{-12}
d_{31} $(Coulomb/Newton)$	-320×10^{-12}	-33×10^{-12}
g_{33} $(Volt-meter/Newton)$	19×10^{-3}	-216×10^{-3}
g_{31} $(Volt-meter/Newton)$	-9.5×10^{-3}	330×10^{-3}
Young modulus (Pa)	-9.5×5^{10}– 6.2×5^{10}	2×2^{9}– 4×2^{9}

The manufacturing method used in fabrication of these tactile sensors are layer by layer method. The proposed sensor is comprised of five layers. on layer of sensing element which are 3x3 matrix of PZT or PVDF taxels. 2 layers of electrodes which are connected to the top and bottom of sensing elements and two layers of Ecoflex 30

silicone coating (Figure 2.3). The reasons why silicone is used in sensor design are: making the sensor more impact resistant, more compact and wearable. In PZT type piezoelectric sensor, since the sensing elements are fragile, silicone coating has more significant function. This coating increases the amount of applicable force ranges on the sensor and protects PZTs from breaking.

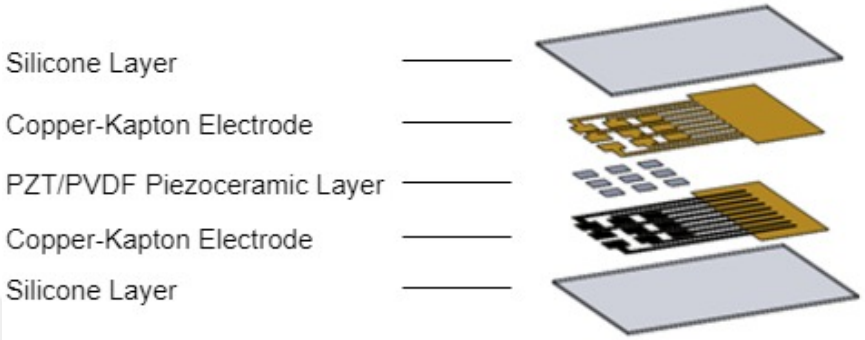

Figure 2.3 : Layers of proposed tactile sensors.

When the force is applied on the sensors, the taxels produce signals and according to the signal amplitudes, the position and magnitude of the force is estimated. However, Signals produced by the sensors, have to be distinguishable and measurable with provided data acquisition card (cDAQ-9174, NI-9220). By taking account all of these limitations, it is observed that two factors affect the output of sensors: silicon coating thickness and the distance between two adjacent taxels. Silicone thickness, has direct influence on the induced charge by affecting force applied on the taxels. In sensor design, generating more charge for the same amount of force is desired. Since by producing more charge, more voltage is obtained and it leads to achieve sensors with higher resolutions. The other parameter is related about distance between taxels. By increasing this distance, non-sensitive regions appear. This means that by applying force on these regions, taxels do not produce any signals and sensor will not detect the position and amount of the force. To obtain the optimal values for these factors, finite element model of for a single taxel coated with silicone is developed.

2.1 Silicone Thickness Analyses

In this section, the voltage output of a single taxel for two different sensing element (PZT PSI-5H4E and PVDF) embedded in Ecoflex 30 has been investigated. A

two dimensional (2D) Finite element method (FEM) model of each taxel has been developed in COMSOL Multiphysics (Figure 2.4). In these analyses plane stress 2D approximation has been used. Silicone is considered as a hyperelastic material and Yeoh model coefficients are taken from [49]. The size of taxel is considered as 4x4 mm square. The thickness of silicone layers is 'k' and 'f' is the amount of total impulsive force applied as homogeneous pressure. Variable 'k', take values from 0 mm to 3 mm with steps of 0.5 mm in each analysis whereas 'f' varies from 0.2 N to 1 N.

In PZT based taxel analyses, the thickness of PZT is 0.127 mm. PZT coefficients such as stiffness, dielectric and piezoelectric constants are provided by manufacture (PIEZO SYSTEMS, INC.). Voltage output is the magnitude of maximum voltage of the taxel with silicone thickness of 'k', when total applied force is 'f'. The results of these analyses are plotted in Figure 2.5.

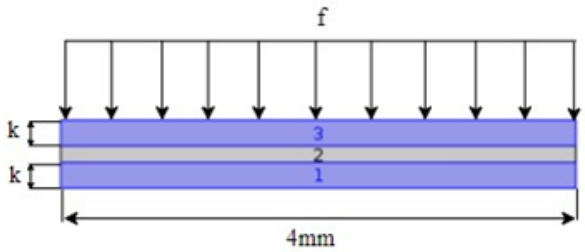

Figure 2.4 : 2D view of taxel with PZT/PVDF sensing element (part2) embedded between two layers of ecoflex30 (1 and 3).

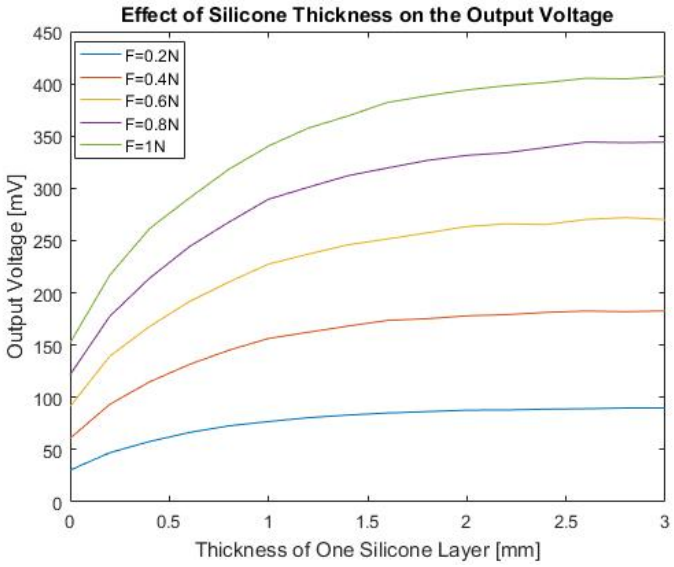

Figure 2.5 : Effect of silicone thickness on output voltage of PZT based tactile sensor.

For PVDF based tactile sensor, same analyses have been done (Figure 2.5). Thickness of PVDF layer is 52 micrometers. Thickness of silicone layer is 'k' where the applied total force is 'f'. 'k' and 'f' takes values from 0 mm to 3 mm with step size of 0.5 mm and 0.2 N to 1 N with steps of 0.2 N respectively.

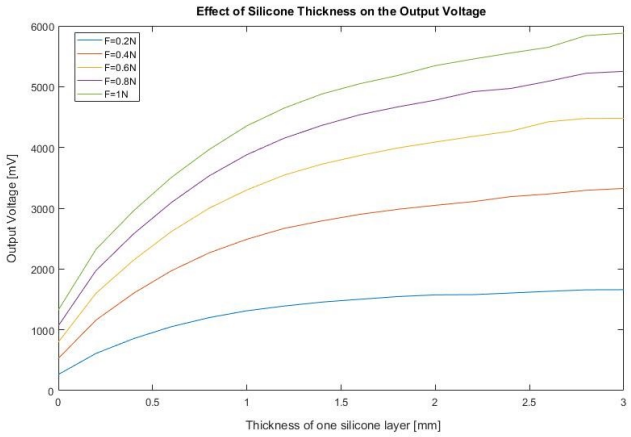

Figure 2.6 : Effect of silicone thickness on output voltage of PVDF based tactile sensor for varied force.

According to Figure 2.5 and 2.6 it can be seen that by increasing the silicone layer of the sensors, the voltage produced by the taxels are increased. However, the rate of this change, decreases. By considering flexibility and wearability of these sensors, silicone layer thickness of 1 mm have been chosen. This make the sensors to have thickness of 2 mm.

2.2 Analyses of Distance Between Taxels

As it mentioned before, force localization is one of the tasks defined for these sensors. In order to study the behavior of adjacent taxels to a known applied force, these analyses have been conducted. Like silicone thickness analyses, a 2D model with plane stress approximation has been created. The model contains two taxels coated with Ecoflex30 (Figure 2.7) and the distance between them is named as parameter 'd_i'. The force 'f' is applied as a homogeneous pressure on a taxel and by varying the amount of force 'f' and distance 'd_i' in each analysis, the behavior of voltage output of adjacent taxel has been studied. 'f' has ranges from 0.2 N to 1 N with step size of 0.2 N whilst 'd' varies from 1 mm to 5 mm with step size of 0.5 mm.

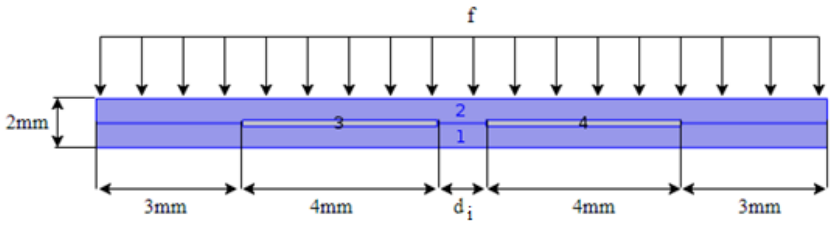

Figure 2.7 : Two taxels with distance 'd_i' embedded in of ecoflex30 (1 and 3).

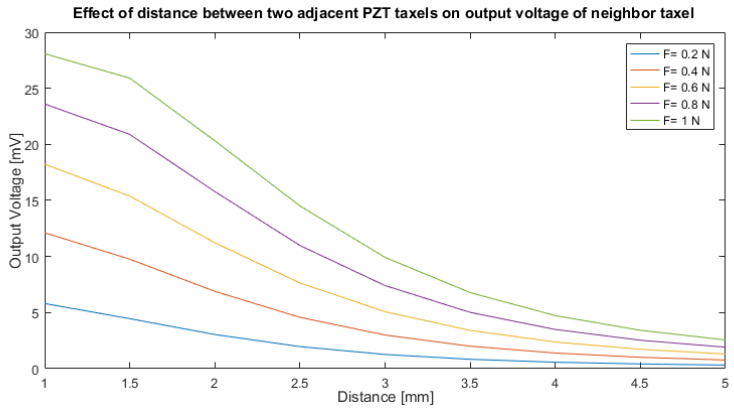

Figure 2.8 : Effect of distance between two adjacent PZT taxels on output voltage of neighbor taxel for varied force.

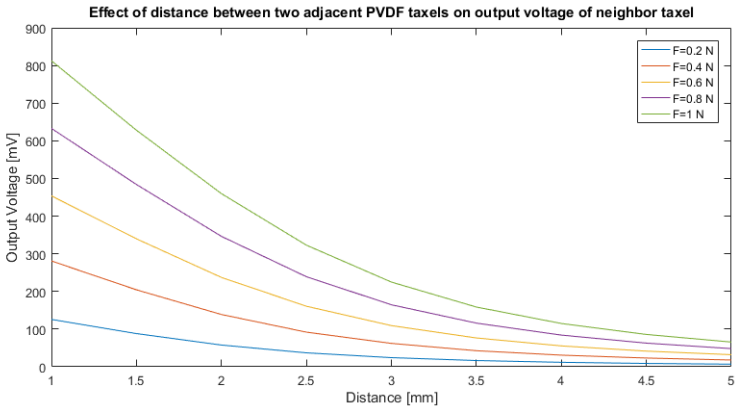

Figure 2.9 : Effect of distance between two adjacent PVDF taxels on output voltage of neighbor taxel for varied force.

Figure 2.8 and Figure 2.9 show that when the distance between two taxels are increased, the voltage magnitude of neighbor taxel decreases. By considering manufacturing limitations and space needed for voltage lines of electrodes, the distance between taxels are selected as 3 mm.

2.3 Manufacturing

In the production of the proposed sensors, layer by layer manufacturing method have been used. The developed tactile sensors are composed of multiple layers: two layers of electrode, one layer of sensing element and two layers of Ecoflex 30 coating. One of the electrode layers used in this sensor is common ground electrode and by measuring the voltage difference at the terminals of the electrodes, amount and position of the applied force can be estimated. PZT and PVDF are two different types of taxels used in this project. Even though the manufacturing process of the electrodes and silicones are same, the production procedure of these sensors are distinct from each other.

2.3.1 PZT based tactile sensor manufacturing

As previously noted, the sensing elements in the proposed tactile sensors are PZT piezoceramics. These PZT piezos are cut in 4mmx4mm dimensions and coated with silver layer. The PZTs are placed in the middle of two layers of electrodes which are made from Pyralux (Copper-Kapton) material.

Both PZT and PVDF type sensors are embedded in silicone. Each layer of silicone has 1 mm thickness and the total thickness of sensor is 2 mm. In order to make the silicone coating, a suitable mold is designed and printed by 3D printer (Figure 2.10.a). After this step, two parts of Ecoflex silicone is mixed in a suitable pot (Figure 2.10.b). Then, the pot is placed in vacuum chamber for 5-10 minutes (Figure 2.10.c). The reason of this step is to minimize the number of bubbles created during mixing procedure and having more homogeneous silicone. After de-airing the silicon mixture, it is ready for potting process (Figure 2.10.d). In the following, silicone in poured into the mold and it is put in vacuum chamber for 5-10 minutes again (Figure 2.10.e). The cure time of Ecoflex30 is 4 hours. After this amount of time, silicone layers are ready to be removed from the mold. (Figure 2.10.f)

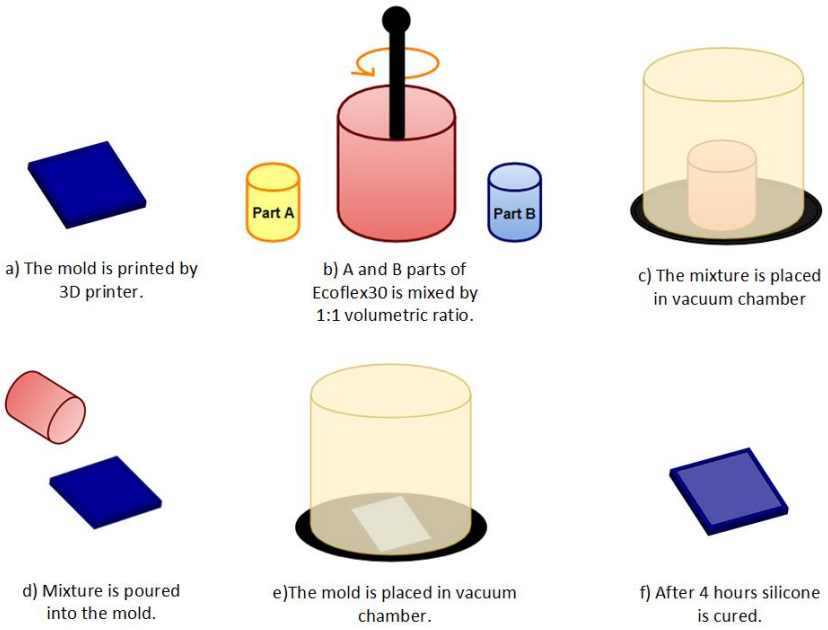

Figure 2.10 : Manufacturing steps of silicone manufacturing.

The dimensions and circuit plan of the electrodes are presented in Figure 2.11. At first step of electrode manufacturing, the copper-kapton layer is colored with black paint (Figure 2.12.a). After that, with help of laser cutter machine the pattern of electrodes is created. In this stage, while the pattern of electrodes remains colorful, the paint is removed from the cut sheet (Figure 2.12.b). The next step is etching copper from patterned copper-kapton sheets. The solvent used for etching process is H2O2 (Hydrogen peroxide) and HCl (Hydrogen Chloride) solution with ratio of one to three. During the etching process, the solution reactions with copper present in Copper-Kapton pieces. In this step, the paint prevents reaction between copper and the solution. Due to this reason, the copper underneath the electrode paths remains (Figure 2.12.c). In the following, the outline of the electrodes is cut with help of laser cut machine (Figure 2.12.d). On the electrode paths, there are 4x4 mm squares which PZT elements are attached on it. In order to attach the PZTs to the electrodes, the paint of these regions are removed. The dimensions of these regions are 2x2 mm squares that are smaller than the PZT attachment area of the electrodes. The reason of that is to decrease the possibility of short circuiting of PZTs during gluing with epoxy (Figure 2.12.e). After this step, the cables are attached to the electrodes (Figure 2.12.f). Then, PZTs are attached to the electrodes with epoxy. To speed up cure time of the epoxy, the electrodes can be placed in furnace in 100°C for 15 minutes (Figure 2.12.g). In the following, the other electrode layer is attached with the same process. (Figure 2.12.h)

Finally, 2 parts of Ecoflex 30 is mixed and spread on the inner surfaces of silicone and the sensor is placed in the middle of the silicone layers. After 4 hours, the top and bottom layers of the silicone are bonded together and the sensor comes to the final form. (Figure 2.12.i)

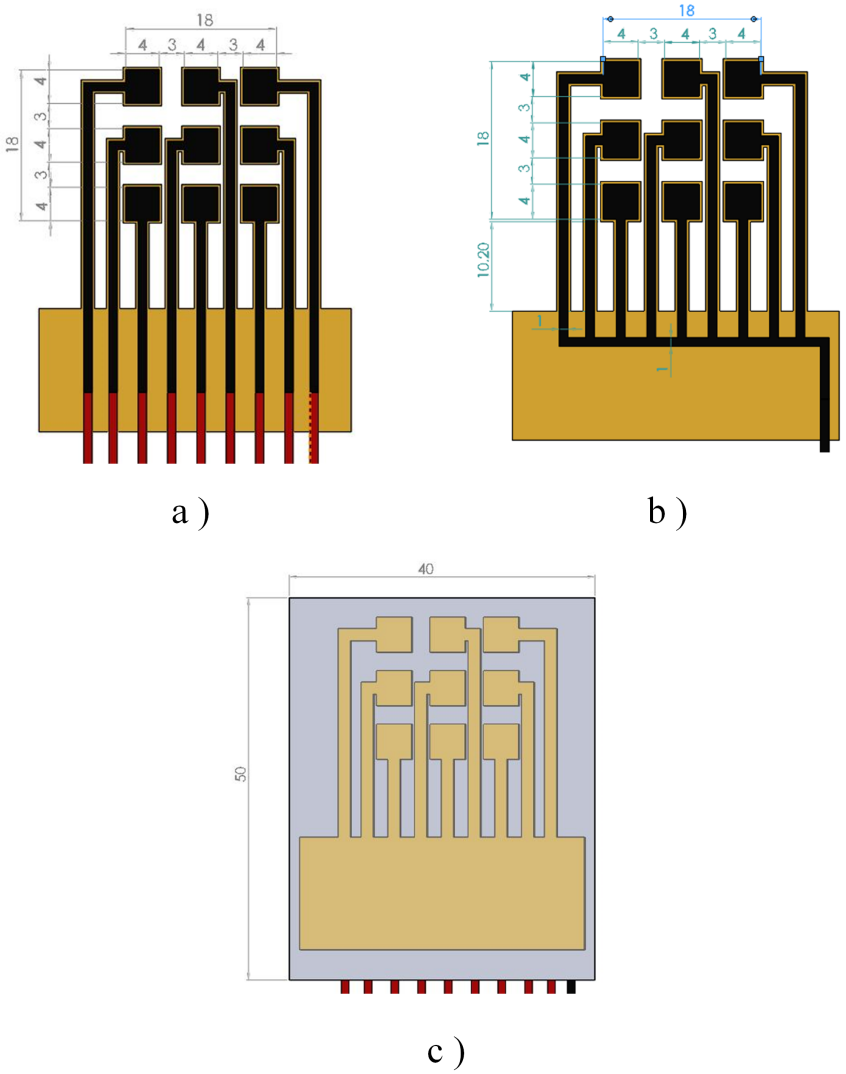

Figure 2.11 : a) and b) dimensions of electrode layer. c) Final dimension of tactile sensor [mm].

a) Copper-Kapton sheets are cut and colored with black paint.

b) With help of laser cutting machine the paint is removed from the sheet and desired pattern for electrodes are obtained

c) The patterned sheet, is etched with HCL and H_2O_2 solution (Ratio 3:1).

d) Outline of the electrodes are cut by laser cutting machine.

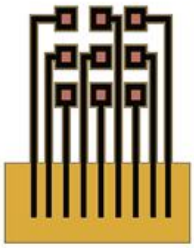

e) In order to attach PVDF to the electrodes, by help of laser cutting machine, paint is removed from the electrodes as 2x2 mm squares.

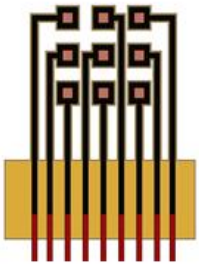

f) Cables are soldered to the terminal of the electrodes.

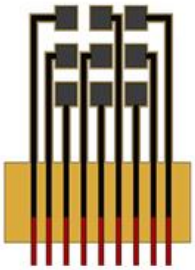

g) PZTs are attached to the electrodes by epoxy.

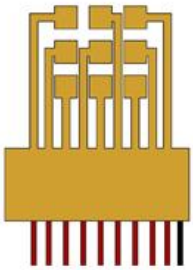

h) the other electrode layer is attached.

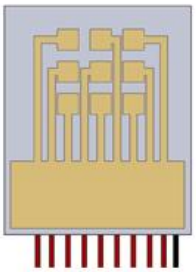

i) Sensor is coated with silicone.

Figure 2.12 : PZT based sensor manufacturing.

2.3.2 PVDF based tactile sensor manufacturing

The process of electrode and silicone making of the sensor is same for both types of PVDF and PZT sensors (Figure 2.13.a- 2.13.f). As it mentioned before, the only difference in fabrication of these sensors are related to utilize distinct sensing element materials. PVDFs are coated with two layers of silver ink electrodes. Cutting PVDF piezo is not an undemanding process. The silver ink layers of PVDF are extremely thin (less than 52 micro meters). So during the cutting, the probability of short circuit of PVDF because of contact between top and bottom surfaces are high. Owing to this fact, to prevent this contact one side of PVDF is etched with acetone. Similar to PZT based tactile sensor, in the fabrication of PVDF sensors, there is a common ground layer. Due to this reason, the surface which is attached to the common ground electrode, should not be etched. So, in order to remove silver ink layer from only one surface of PVDF, one side of PVDF is washed with acetone whilst the other side is banded with tape to prevent etching (Figure 2.13.g and 2.13.h). In the following steps, silver ink coated side of PVDF is attached to the common ground electrodes and coated with silicone (Figure 2.13.i - 2.13.k).

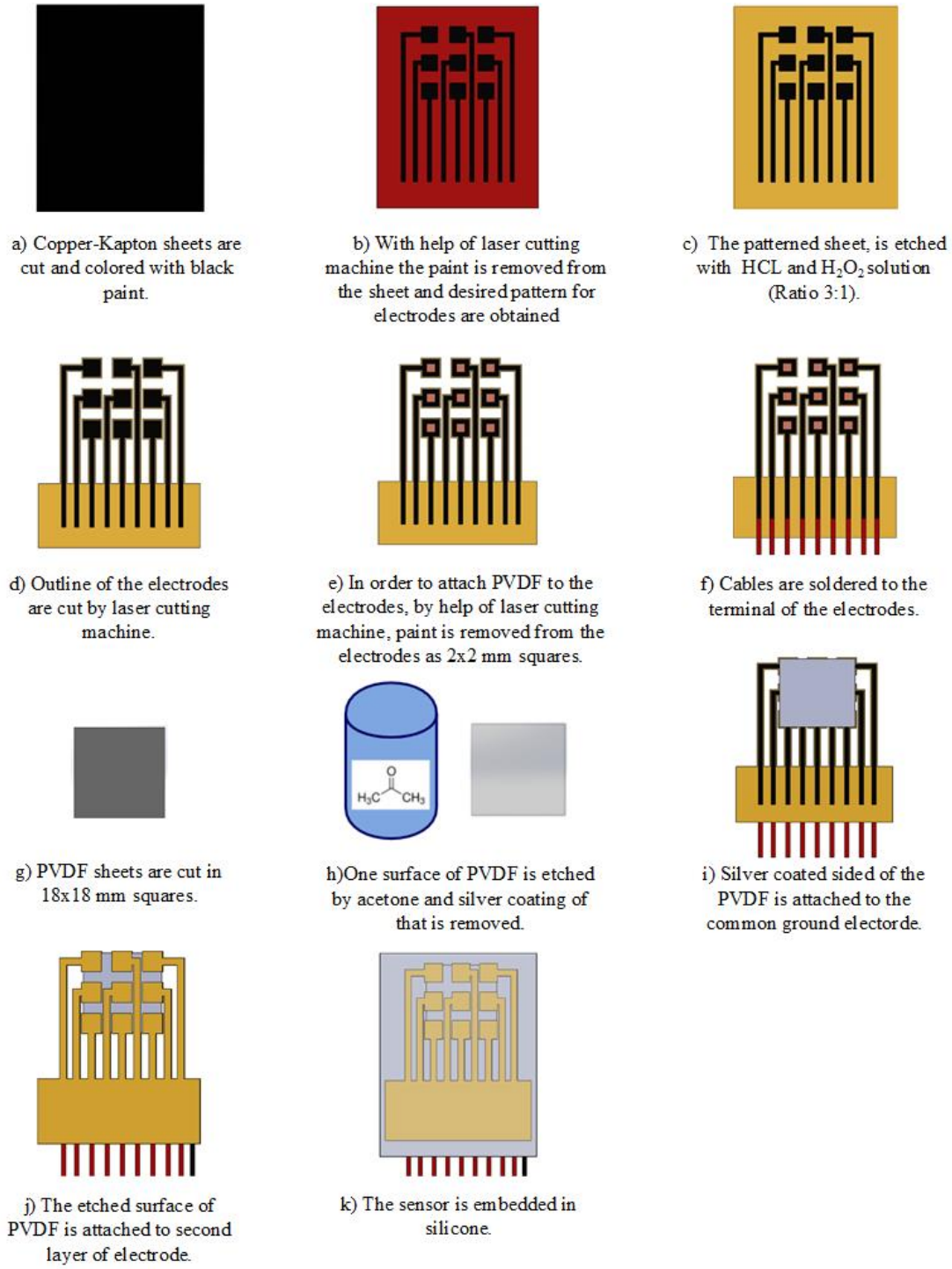

Figure 2.13 : PVDF based sensor manufacturing.

3. THEORETICAL AND FEM MODELING OF TACTILE SENSOR

All of the materials have stiffness and damping properties which can be expressed by equivalent spring and dampers. As a result, the mechanical behavior of the most materials can be modeled as mass-spring-damper model. Silicone and piezoelectric materials are not excluded from this fact. Thus, 3 DoF mass-spring-damper system is proposed to estimate sensor's voltage behavior of single taxel coated in silicone to the applied force (Figure 3.1). When a piezoelectric material is subjected to a dynamic normal force, the embedded piezo element is deformed in elastic region and this deformation led to the generation of electrical charge by the sensing element. In the first part of this section, the relation between the charge accumulated in piezoelectric and the applied force is obtained and the second part is related to the modeling of charge amplifier circuit used for amplifying the induced charge of piezoelectric.

3.1 State Space Model of Induced Electrical Charge in Single Taxel

As it mentioned before, a single piezo element embedded in silicone can be simplified as 3 degree of freedom mass-spring-damper system (Figure 3.1).

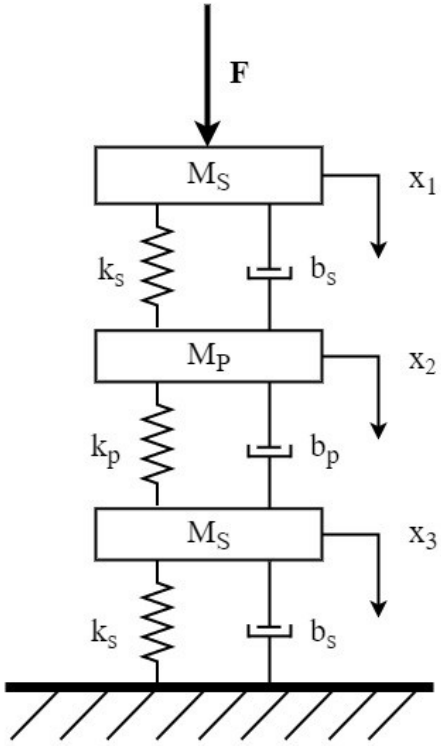

Figure 3.1 : Mass-spring-damper model of single taxel.

Figure 3.2 represents the free body diagram of the top silicone layer of the sensor. 'X_1', 'X_2' and 'X_3' are the displacement amount of the top silicone layer, piezoelectric and bottom silicone layer respectively. According to Newton's second law:

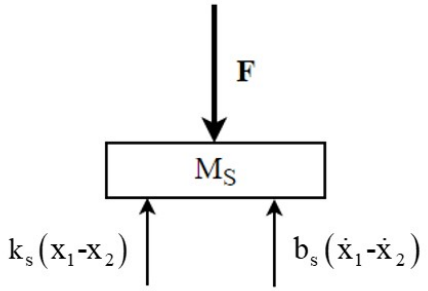

Figure 3.2 : free diagram body of the top silicone layer.

$$\sum f = m_s \ddot{X}_1 \tag{3.1}$$

$$F - k_s(X_1 - X_2) - b_s(\dot{X}_1 - \dot{X}_2) = m_s \ddot{X}_1 \tag{3.2}$$

Where 'f' is applied normal force on sensor,'M_s','k_s 'and 'b_s' are the mass, stiffness and damping coefficients of the silicone layer with 4x4 mm surface area 'A_s' and 1 mm thickness 't_s'. These properties can be calculated like below [46]:

$$M_s = \rho_s t_s A_s \tag{3.3}$$

$$b_s = \frac{\mu_s}{t_s} A_s \tag{3.4}$$

$$k_s = \frac{E_s}{t_s A_s} \tag{3.5}$$

where 'μ_s' and 'E_s' represent viscosity and elastic modulus of the silicone layer.For the piezoelectric element we have:

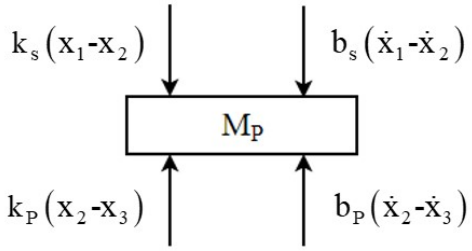

Figure 3.3 : Free diagram body of the piezoelectric layer.

$$k_s(X_1 - X_2) + b_s(\dot{X}_1 - \dot{X}_2) - k_p(X_2 - X_3) - b_p(\dot{X}_2 - \dot{X}3) = m_p\ddot{X}_2 \tag{3.6}$$

In above equation, 'M_p', 'k_p' and 'b_p' are mass, stiffness and damping coefficients of the piezo element. mass and stiffness of the piezoelectric, similar to silicone layer can be calculated by equations 3.3 and 3.5 . Finally the equation motion of bottom silicone layer can be written like below:

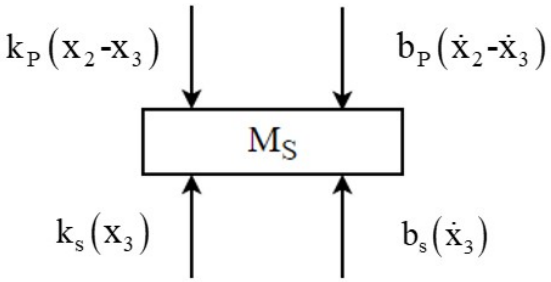

Figure 3.4 : Free diagram body of the bottom silicone layer.

$$k_p(X_2 - X_3) + b_p(\dot{X}_2 - \dot{X}_3) - k_s X_3 - b_s \dot{X}_3 = m_s \ddot{X}_3 \tag{3.7}$$

By assuming all initial conditions as zero, state space model of sensor can be obtained. The output of this sensor is the amount of piezo deformation. This value is equal to difference between displacements of piezoelectric and bottom silicone layers. By multiplying deformation amount by kp, the applied force applied on the piezo electric

can be found.

By defining the states in equation 3.8:

$$X = \begin{bmatrix} x_1 \\ x_2 \\ x_3 \\ x_4 \\ x_5 \\ x_6 \end{bmatrix} = \begin{bmatrix} x_1 \\ \dot{x}_1 \\ x_2 \\ \dot{x}_2 \\ x_3 \\ \dot{x}_3 \end{bmatrix} \tag{3.8}$$

The state space representation of a system are:

$$\dot{X} = AX + Bu$$

$$Y = CX + Du$$

Therefore, by considering equations 3.2, 3.6and 3.7,the 'A', 'B', 'C' and 'D' matrices of the state space model can be obtained:

$$A = \begin{bmatrix} 0 & 1 & 0 & 0 & 0 & 0 \\ -k_s/m_s & -b_s/m_s & k_s/m_s & b_s/m_s & 0 & 0 \\ 0 & 0 & 0 & 1 & 0 & 0 \\ k_s/m_p & b_s/m_p & -(k_s+k_p)/m_p & -(b_s+b_p)/m_p & k_p/m_p & b_p/m_p \\ 0 & 0 & 0 & 0 & 0 & 1 \\ 0 & 0 & k_p/m_s & -(b_s+b_p)/m_s & -(k_s+k_p)/m_s & -(b_s+b_p)/m_s \end{bmatrix} \tag{3.9}$$

$$B = \begin{bmatrix} 0 \\ 1/m_s \\ 0 \\ 0 \\ 0 \\ 0 \end{bmatrix} \tag{3.10}$$

In the state space model, the input of system is f and the output is the charge induced in piezoelectric. Thus: $f = u$ and $Y = Q$. The difference between 'x_2' and 'x_3' is the elongation amount of piezoelectric. So, by dividing this value to the thickness of the piezoelectric material, strain can be calculated:

$$s = (x_2 - x_3)/t_p \tag{3.11}$$

By neglecting strains in other directions, the induced charge can be obtained:

$$Q = e_{33}.s.A_p \tag{3.12}$$

Therefore, 'C' and 'D' matrices of state space model are:

$$C = \begin{bmatrix} 0 & e_{33}.A_p/t_p & -e_{33}.A_p/t_p & 0 & 0 & 0 \end{bmatrix} \tag{3.13}$$

$$D = 0 \tag{3.14}$$

3.2 Transfer Function of Charge Amplifier

All the cables and electrodes used in sensors have various internal resistance and capacitance which affect output signal of the sensors. In piezoelectric based tactile sensor, due to high impedance of piezoelectrics, the effect of resistance and capacitance of cables are more significant. In order to solve this problem, an additional charge amplifier circuit is needed.

Figure 3.5 demonstrates equivalent circuit of piezoelectric sensor connected to charge amplifier. In this circuit, 'Q_p' is the electric charge of piezoelement produced by mechanical force or vibration and 'C_p','C_c','C_{in}' and 'C_{fb}' are denoting the capacitance of piezoelectric, connecting cables, input of amplifier circuit and feedback circuit respectively. In the same manner, 'R_p','R_c','R_{in}' and 'R_{fb}' are resistances of piezoelectric, connecting cables, input of amplifier circuit and feedback circuit. Owing to high resistance value of amplifier piezoelement input and feedback circuits, the circuit shown is Figure 3.5 can be simplified as Figure 3.6.

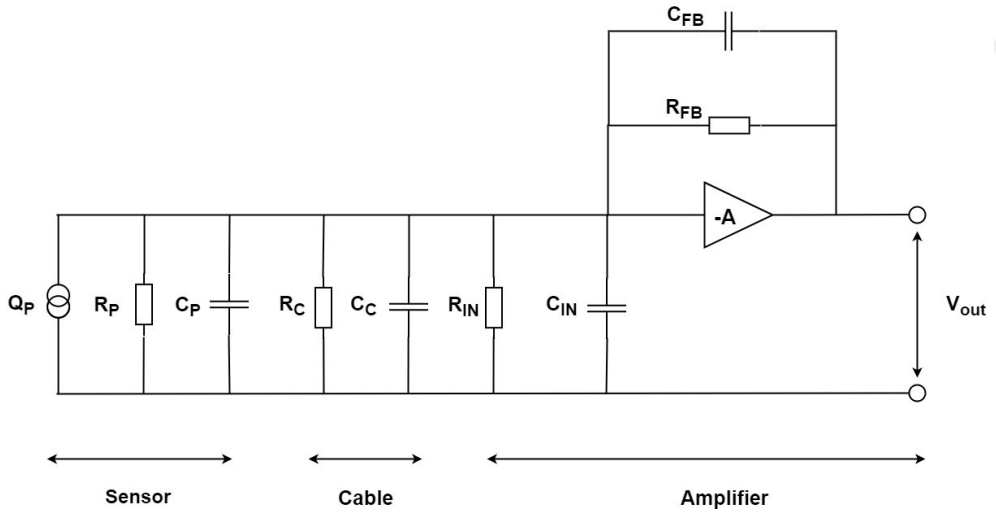

Figure 3.5 : Equivalent electric circuit of charge amplifier connected to piezoelectric sensor.

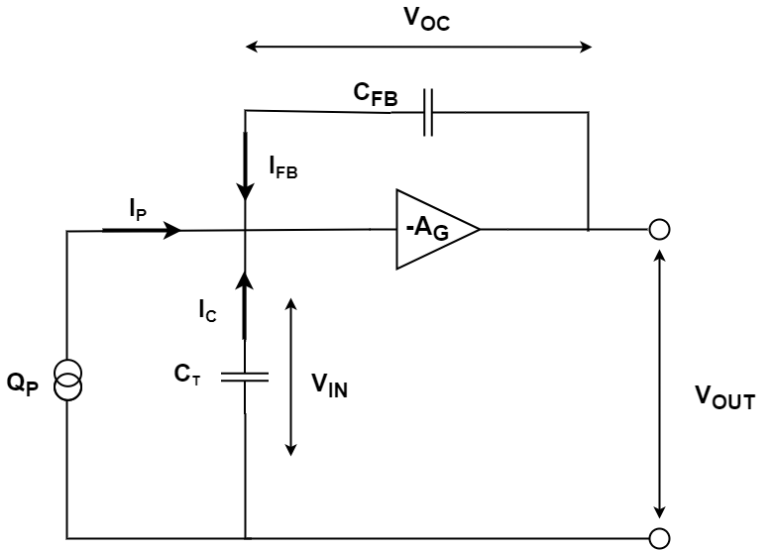

Figure 3.6 : Simplified equivalent electric circuit of charge amplifier connected piezoelectric sensor.

In the the simplified charge amplifier circuit [39]:

$$C_t = C_P + C_C + C_{IN} \tag{3.15}$$

In order to find the relation between charge induced and the output voltage:

$$V_{out} = -A_G V_{in} \tag{3.16}$$

$$V_{FB} = V_{out} - V_{in} = (1 + \frac{1}{A_G}) V_{out} \tag{3.17}$$

$$I_p + I_C + I_{FB} = 0 \tag{3.18}$$

$$I_p = \frac{dQ_p}{dt} \tag{3.19}$$

$$I_{FB} = C_{FB}\frac{dQ_p}{dt} = (1 + \frac{1}{A_G}) C_{FB}\frac{dV_{out}}{dt} \tag{3.20}$$

$$I_C = C_T \frac{dV_{IN}}{dt} = \frac{1}{A_G} C_T \frac{dV_{out}}{dt} \tag{3.21}$$

$$\frac{dQ_p}{dt} = -(1 + \frac{1}{A_G}) C_{FB}\frac{dV_{out}}{dt} - \frac{1}{A_G} C_T \frac{dV_{out}}{dt} \tag{3.22}$$

Finally by taking integral from both sides of 3.22 we have:

$$V_{out} = -\frac{Q_p}{(1 + \frac{1}{A_G}) C_{FB} + \frac{1}{A_G} C_T} \tag{3.23}$$

Since the gain constant of opamps are high, $1/A_G$ term can be neglected. As a result:

$$\frac{V_{out}}{Q_p} = -\frac{1}{C_{FB}} \tag{3.24}$$

3.3 FEM Modeling of Tactile Sensor

In order to study the behavior of the sensor to applied forces and voltage output of taxels, finite element model of sensor have been developed in COMSOL MULTIPHYSICS software. With help of these analysis, the design parameters have been selected. Time dependent and frequency response 2D analyses has been conducted. As it discussed before, the proposed sensors are composed of piezoelements embedded in Ecoflex30. Ecoflex30 is istropic and incompressible hyperelastic material which can be modeled by using non-linear elastic theory. [50].ECoflex30 can be modeled as Yeoh model [51].

$$U = C_{10}(I_1 - 3) + C_{20}(I_1 - 3)^2 + C_{30}(I_1 - 3)^3 \tag{3.25}$$

Where 'U' represents the strain energy per unit of reference volume,'C_{10}', 'C_{20}', 'C_{30}' are the coefficients of the polynomial and the stress invariant is denoted by 'I_1'. The coefficients needed for the analysis are taken from [49]

4. EXPERIMENTS AND RESULTS

4.1 Experimental Setup

As it mentioned before, the goal of this project is to develop a sensor with force measuring and localization ability. In order to investigate these properties, a suitable experimental setup with the capability of applying and measuring various types of force such as impulsive, step-wise and harmonic had to be designed. The experimental setup used for this project is composed of seven types of components (Figure4.1):

- 3 linear stages
- DDLM-019-070-01 direct drive linear actuator
- CyberFet 2x30A DC Motor Controller
- Signal generator/NI
- HBM U9C 50N load cell
- NI cDAQ-9174/9220/9264 and HBM QUANTUM MX840A data acquisition cards
- Signal conditioning unit

As it can be seen in the Figure 4.1 there are two linear stages in horizontal directions which is utilized to place the sensor in the desired position in XY plane. The force applied on the sensor is provided by DDLM-019-070-01 direct drive linear actuator which is mounted on the vertical linear stage. In the actuator used in this project, there is a linear relationship between the current and the output force. Moreover, applying high frequency forces are possible. Desired current signal is generated by NI 9264 and CyberFet 2x30A DC Motor Controller. As a result, the actuator exert a force proportional to the current signal. The applied force on the sensor is measured by HBM U9C 50N load cell which is placed underneath of sensor. The measured force data is collected and recorded by the help of HBM QUANTOMX data acquisition card

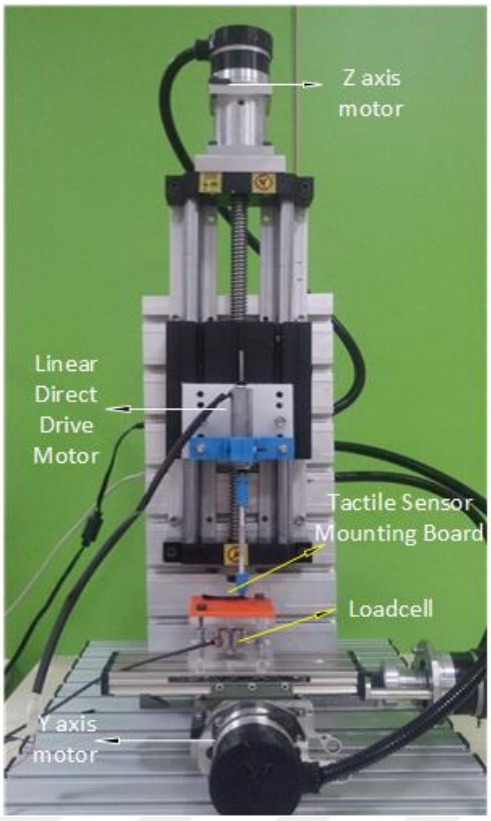

Figure 4.1 : The Experimental test setup.

and CATMAN program. On the other hand, when the sensor is subjected to the force, a voltage signal is generated by the piezoelectric materials . These signals are filtered and amplified by signal conditioning unit and collected by NI9220 DAQ and Labview program.

4.2 Signal Conditioning Unit

Piezoelectric sensors usually have high input impedance and the signals produced by the piezoelectric contain noises and unwanted signals created during the experiment. Moreover, as it noted in section 3.2, the cables used in measurement procedure, have significant effects on the results. Therefore, these signals have to be conditioned before measurement and processing procedure. Charge amplifier and Voltage amplifier are two types of conditioning circuits used in piezoelectric measurements. The charge amplifier's gain is only dependent to the capacitance used in the circuit which makes it more advantageous according to the voltage amplifiers. In contrast, in voltage amplifier circuits, the length of connecting cables affects the output and the circuit has to be calibrated in case of change in length of connecting cables. The conditioning circuit

utilized in this project is the charge amplifier suggested by Texas Instrument (Figure 4.2) [7]:

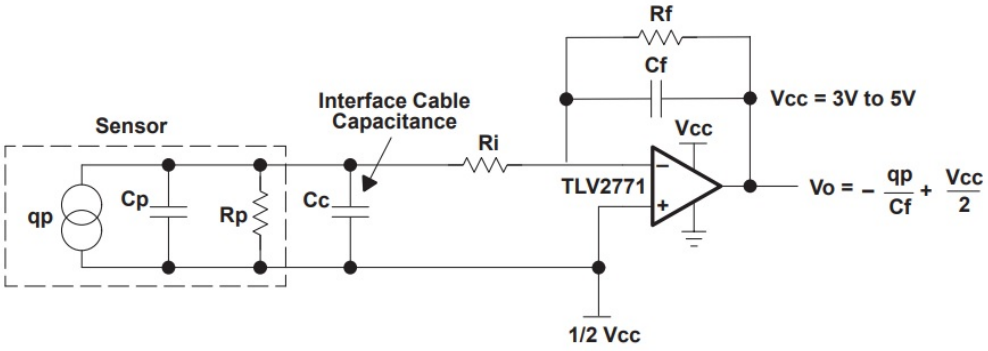

Figure 4.2 : Charge amplifier circuit [7].

This circuit behaves like a band pass filter and the amplification gain is dependent on the frequency Figure 4.3. there are two cutoff frequencies:

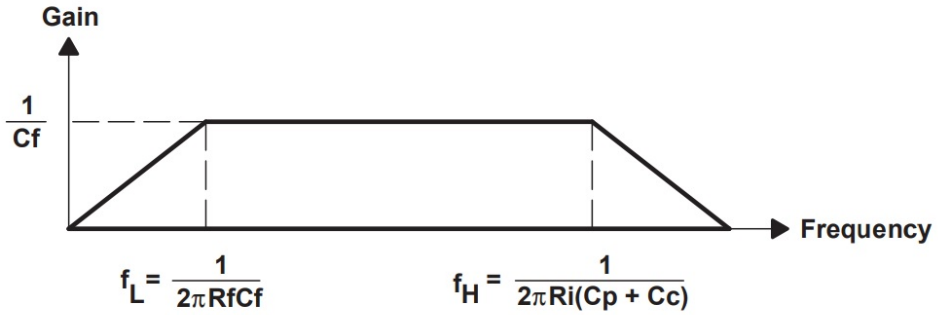

Figure 4.3 : Gain of charge amplifier circuit vs input frequency [7].

as it can be seen from figure above, the higher cutoff frequency is dependent on the capacitance amount of the piezoelectric and the connecting cables. Moreover, high cutoff frequency is a function of input resistance 'R_i'. This resistance provides electrostatic discharge protection. On the other hand, the feedback resistance and capacitance values affect lower cutoff frequency. Preventing amplifier from drifting into saturation and providing a DC bias path for the negative input are the reasons of utilizing feedback resistance in this circuit. It should be noted that sensitivity of the amplifier is inversely dependent on 'C_f'. By changing feedback capacitance value, the lower cutoff frequency varies. Even though by changing 'R_f' cutoff frequency is changed, using feedback resistance greater than 10 M Ω is not suggested due to the

various operational limitations. The values of 'C_f' and 'R_f' have been selected as 820 pF and 10 MΩ respectively.

4.3 Results

In the following sections the force response of taxels has been analyzed and discussed. In the beginning, response of piezoelectric materials to various forces has been studied and frequency response function of the sensor has been obtained. Moreover, the effect of silicon thickness on force response has been experimented. In the following, the results obtained from the experiments are compared with FEM and analytic model. In addition to that, PZT based and PVDF based tactile sensors are compared to each other. Finally, in the last section, localization ability of sensor has been studied.

4.3.1 Step response of piezoelectric material

The first step of studying force response of tactile sensor is studying the force-voltage behavior of single taxel. In order to identify the mathematical model of taxel, step forces are applied on the taxel with help of direct linear motor. Figure 4.4 and 4.5 demonstrate the voltage behavior of piezoelectric taxels to the applied step force. As it can be seen from these figures, both PZT and PVDF behave like a first order system. Thus, by analyzing charging or discharging signals of piezoelectric taxels, the time constant of these taxels can be calculated. It have been observed that even taxels with same sensing element material, are distinct in time constants. These differences are related to impedance differences due to manufacturing errors of piezoelectric materials and taxels. Despite the large variance in time constant and output amplitude of taxels, there is a linear relation between force and output voltage of piezoelectric material taxels (Figure 4.6). Studying step response of the taxels helps us to calibrate the sensors and increase the ability of force measuring and force localization.

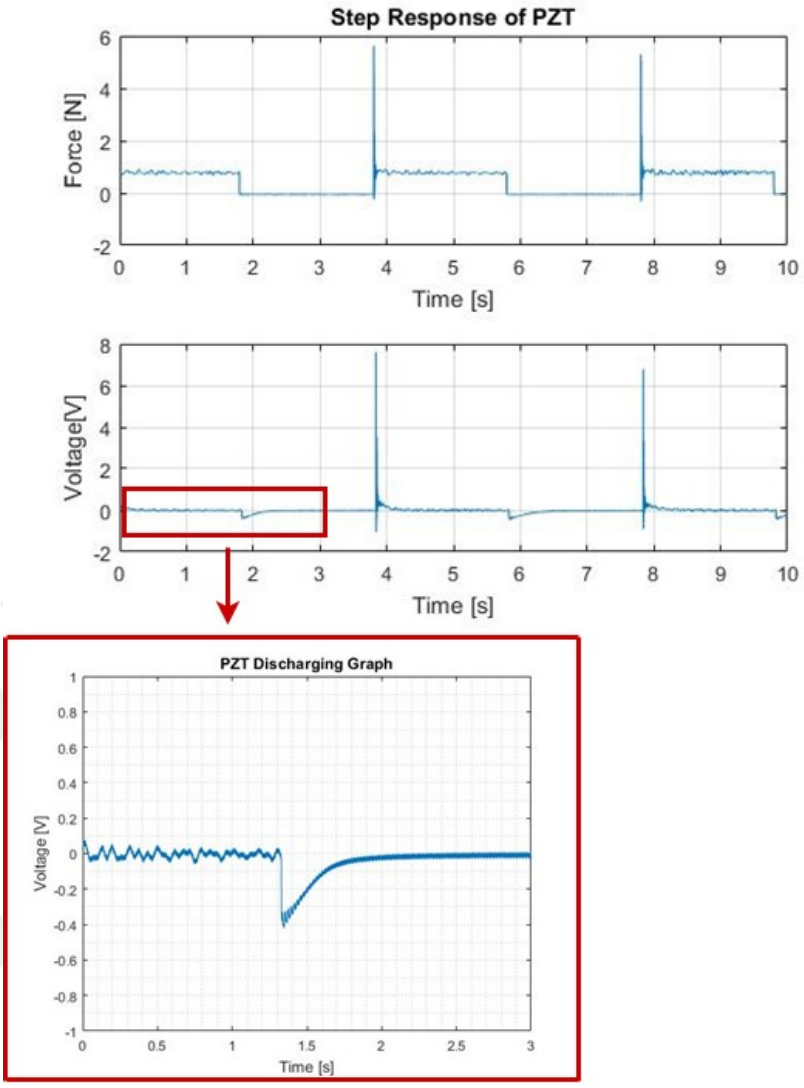

Figure 4.4 : Voltage behavior of PZT piezoelectric material to applied step force.

As it can be seen from the Figure 4.4 and Figure 4.5 , a periodic step force is applied on the taxels. By averaging peak value of discharge signals Figure 4.6 have been obtained. As it mentioned before, there is a linear relationship between force and piezoelectric voltage output.

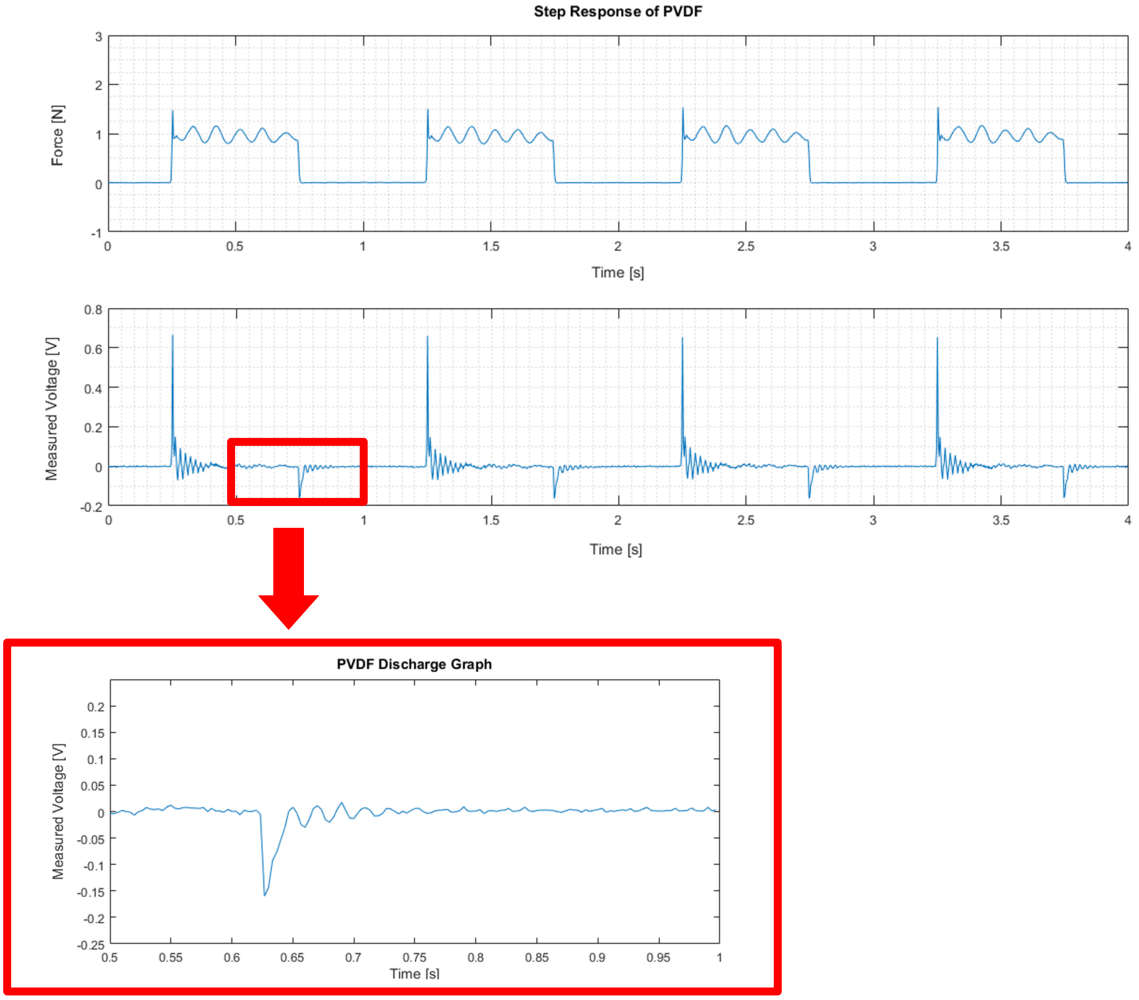

Figure 4.5 : Voltage behavior of PVDF piezoelectric material to applied step force.

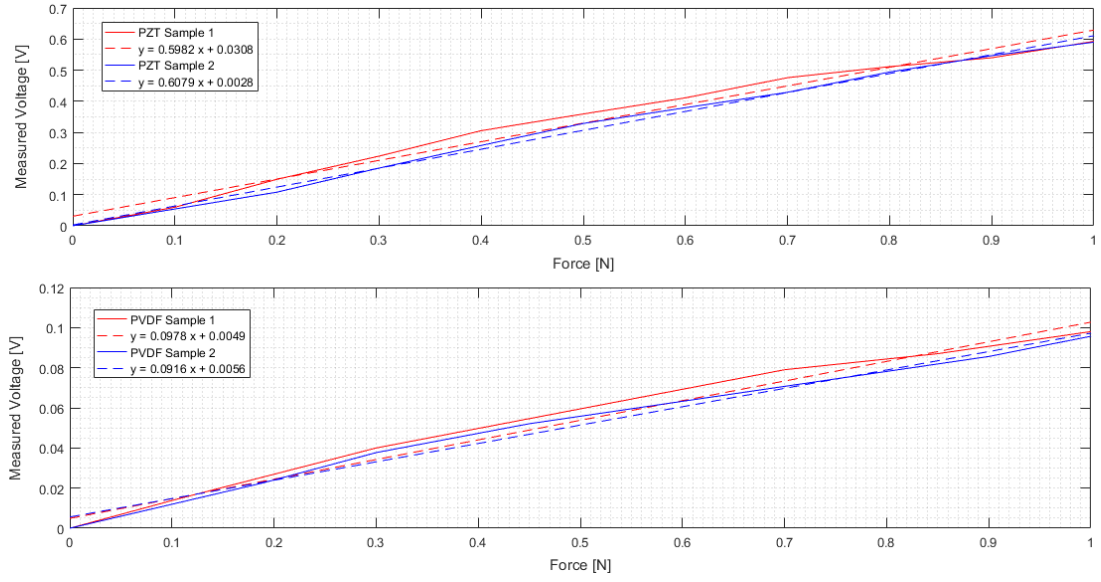

Figure 4.6 : Relationship between force and output voltage of PZT (top) and PVDF (bottom) piezoelectrics.

The correlation coefficient of PZT and PVDF based tactile are calculated as 0.9942 and 0.9933 respectively which demonstrate excellent linearity behavior of the proposed sensors.

4.3.2 Impulse response of piezoelectric material

In this section the response of piezoelectric taxels to the applied impulsive forces have been examined (Figure 4.7). It has been observed that the time response of both types of piezoelectric materials are similar in shape(Figure 4.8 and 4.9).

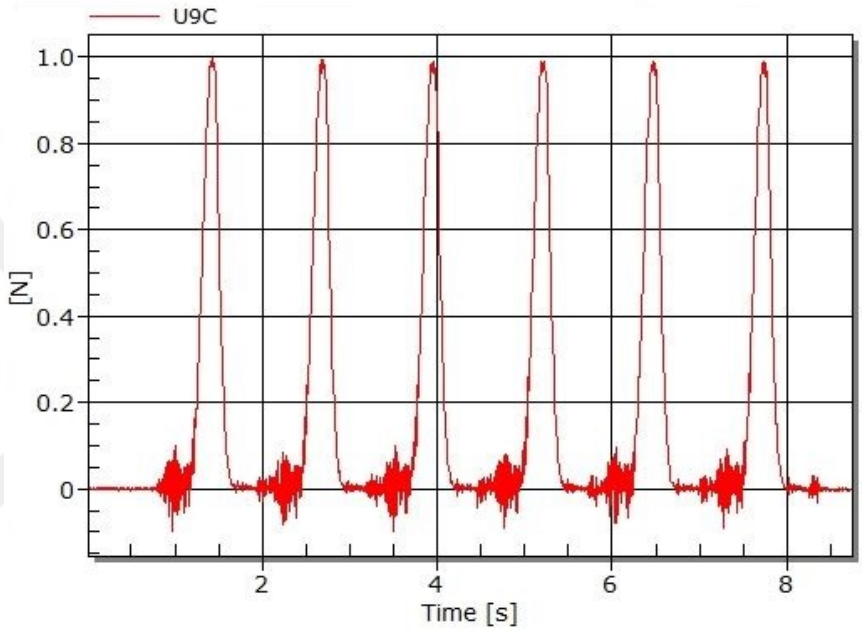

Figure 4.7 : The impulsive force applied on piezoelectric material.

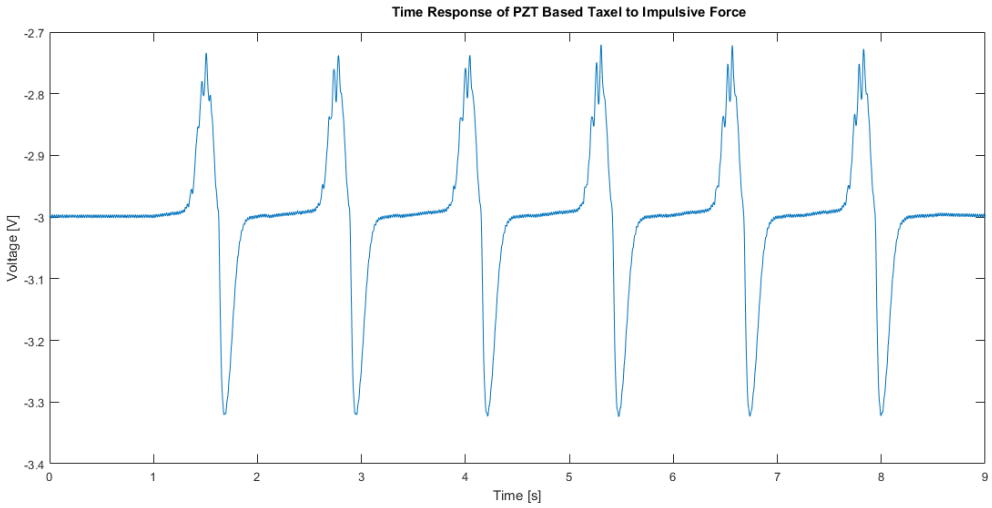

Figure 4.8 : The time response of PZT taxel to impulsive force.

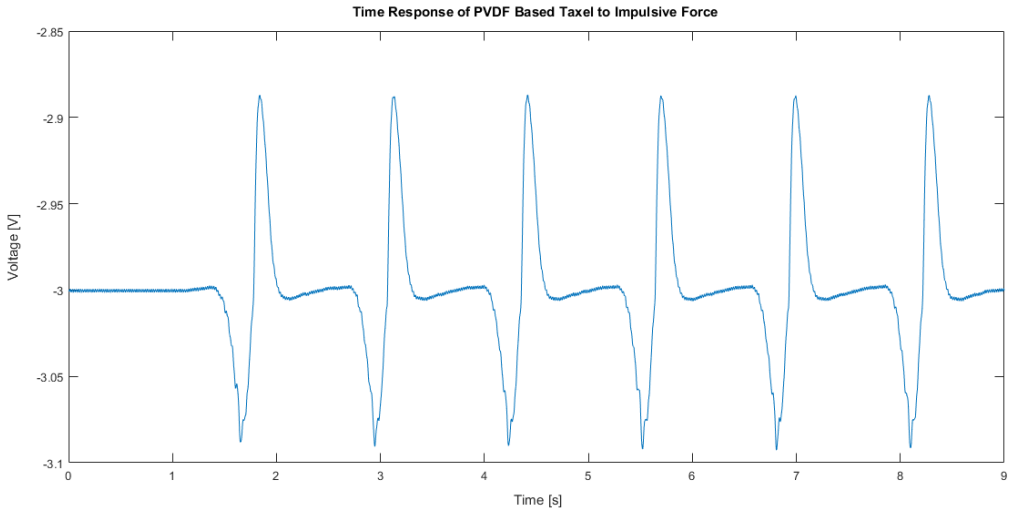

Figure 4.9 : The time response of PVDF taxel to impulsive force.

4.3.3 Frequency response of piezoelectric material

In the second types of analysis, frequency response of piezoelectric materials have been studied. In order to achieve this goal, piezoelectric taxels are subjected to chirp forces. The reason of preferring chirp signal as excitation force type is ability of spanning continuously of all frequency range of interest [52]. Chirp signals are produced by help of NI DAQ card and transmitted to direct linear drive motor by CyberFet 2x30A DC motor controller. The produced chirp signal has initial and final frequency of 0 and 100 Hz respectively for a duration of 8 seconds (Figure 4.10) .

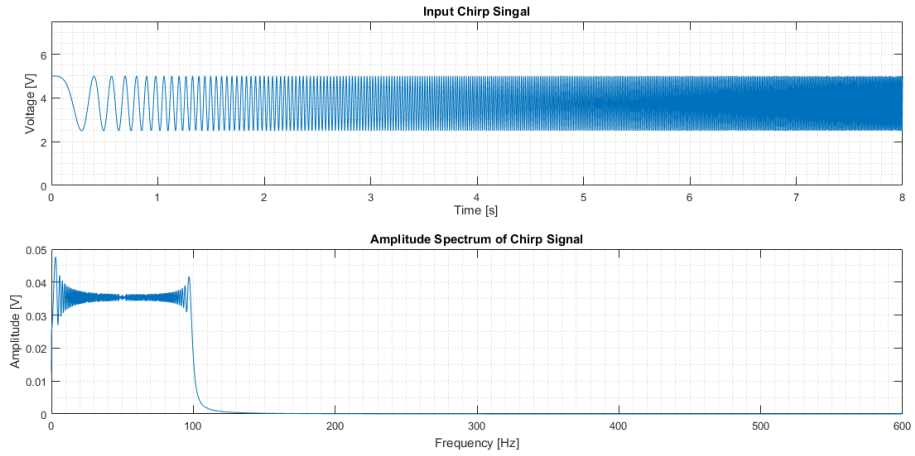

Figure 4.10 : Input chirp signal (top) and its amplitude spectrum (bottom).

The applied force acting on taxel is different from input control signal. Figure 4.11 is the one of the applied chirp force samples. As it can be seen from this figure, even though the amplitude of input control frequency is constant, the amplitude of applied chirp is variant. For example, the amount of force at high frequencies is less than middle and initial frequencies . The reason of this is related to mechanical limitations and frequency response of linear direct motor. In the high frequencies, the acceleration needed for the moving shaft to follow the input signal is high and due to this reason the displacement amount of the shaft decreases and as a result the applied force decreases.

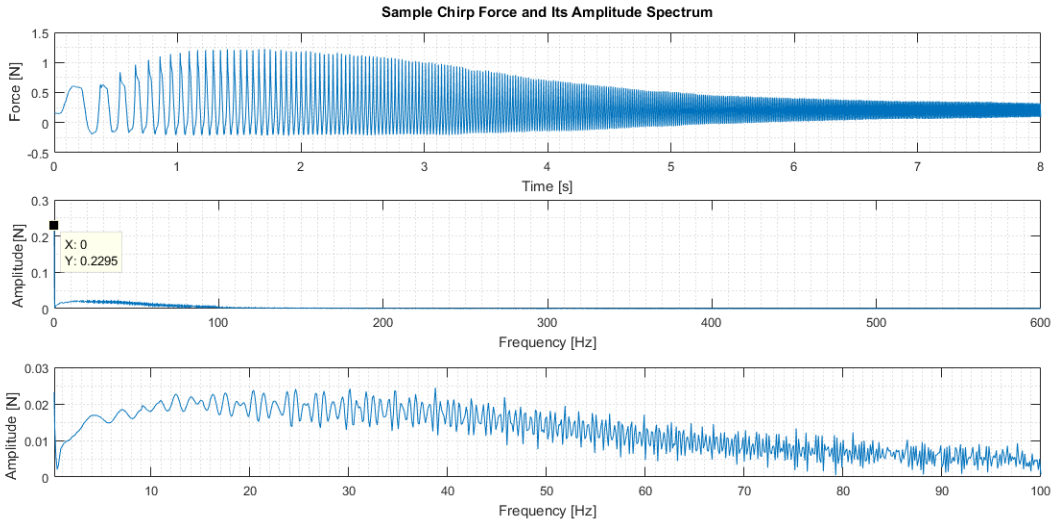

Figure 4.11 : Chirp force applied on the taxels (top) its amplitude spectrum (middle) amplitude spectrum within 0.5 and 100 Hz (bottom).

Figure 4.12 represents the output voltage signal of the PZT taxel sample. By dividing amplitude spectrum of the taxel by amplitude spectrum of the applied force, the frequency response of PZT taxel can be found (Figure 4.13).

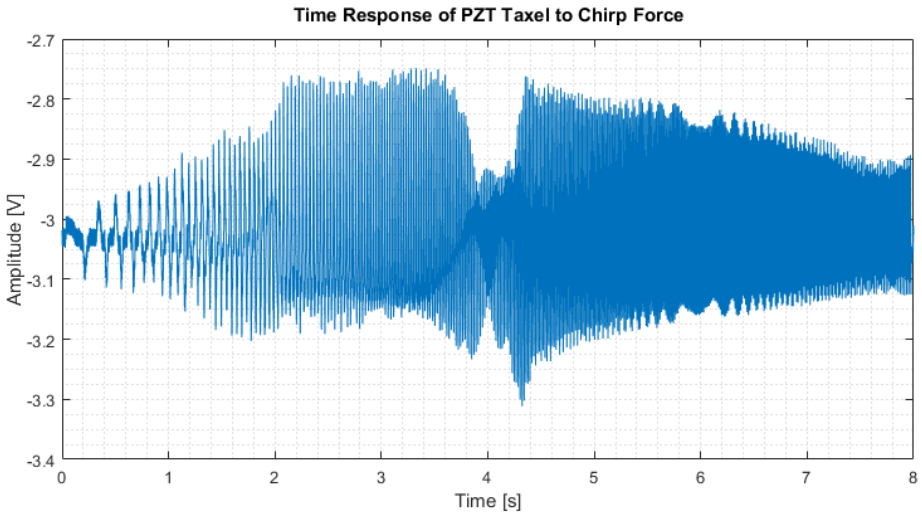

Figure 4.12 : Response of piezoelectric taxel to chirp force.

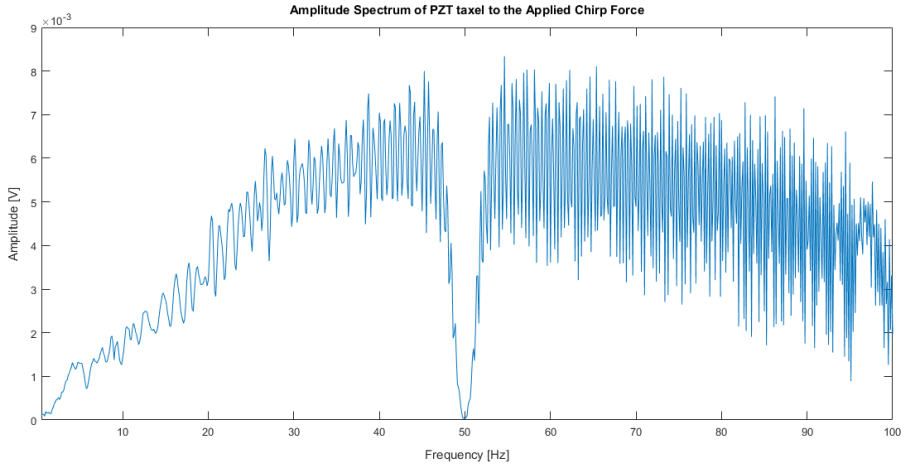

Figure 4.13 : Amplitude Spectrum of PZT taxel response to the applied chirp force.

It has been observed that all the taxels (even taxels with different time constants), exhibit similar frequency response. Figure 4.14 represents the frequency response of two different PZT taxels. In this analysis, in the absence of charge amplifier, the time constant of PZT sample 1 is measured as 3.1 seconds whereas time constant of PZT sample 2 was 1.7 seconds. This measurement procedure is repeated for the PVDF based tactile sensor and the amplitude spectrum for these taxels are obtained. (Figure 4.15)

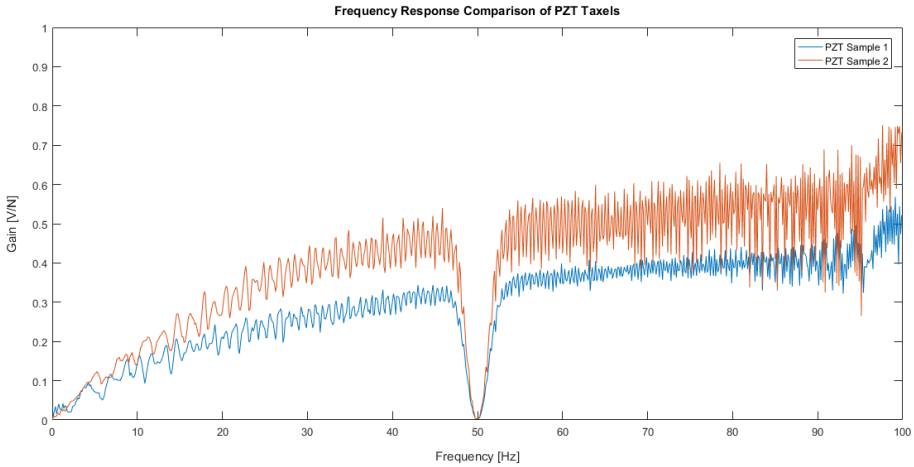

Figure 4.14 : Frequency response of two PZT based taxels.

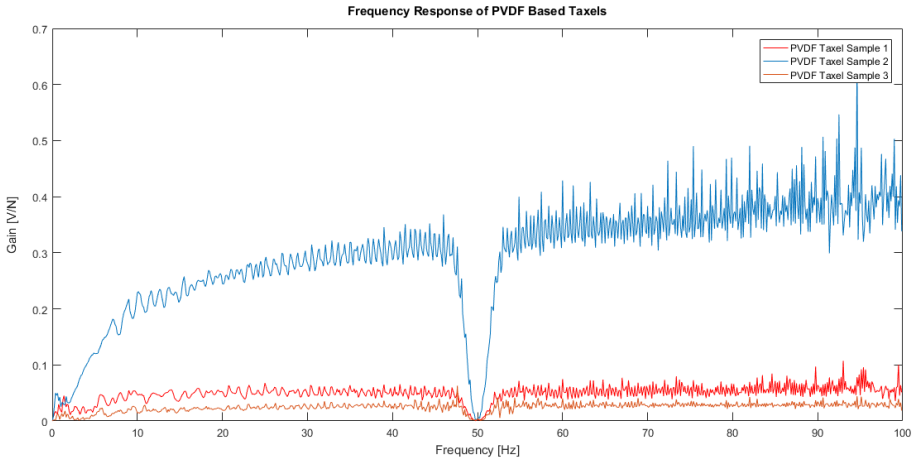

Figure 4.15 : Frequency response of two PVDF based taxels.

As it can be seen from frequency response graphs, in 50 Hz, the gain of taxels is approximately zero. The reason of that is utilizing a second order Butterworth band stop filter in measurements. The effect of using band stop filter in measurements has been plotted in Figure 4.16. These measurements are conducted at different times which shows that repeatability of these measurements.

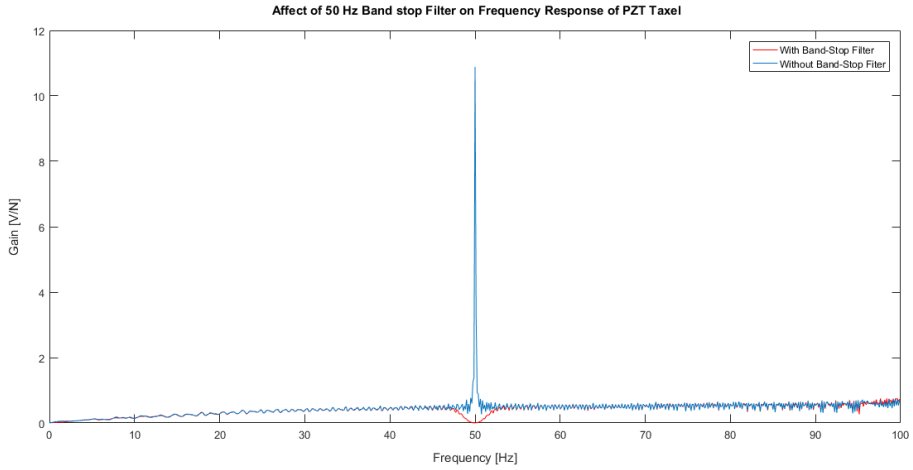

Figure 4.16 : Amplitude Spectrum of PZT taxel response to the applied chirp force.

4.3.4 Repeatability

The proposed sensor has the high amount of repeatability. In this section the taxels have been subjected to periodic impulsive forces and peak values of output voltages have been noted. These experiment have been repeated for 10 times for each taxel. Figure 4.17 and 4.18 are repeatablity test examples of PZT and PVDF taxels. At the end of these tests, the average repeatability factor measured for PZT and PVDF based taxels are calculated as 95.65% and 96.63% respectively.

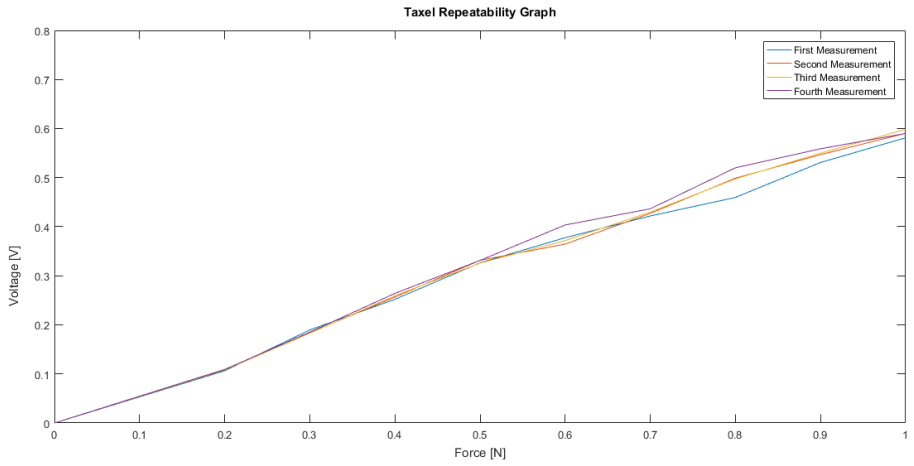

Figure 4.17 : Repeatability graph of PZT taxel.

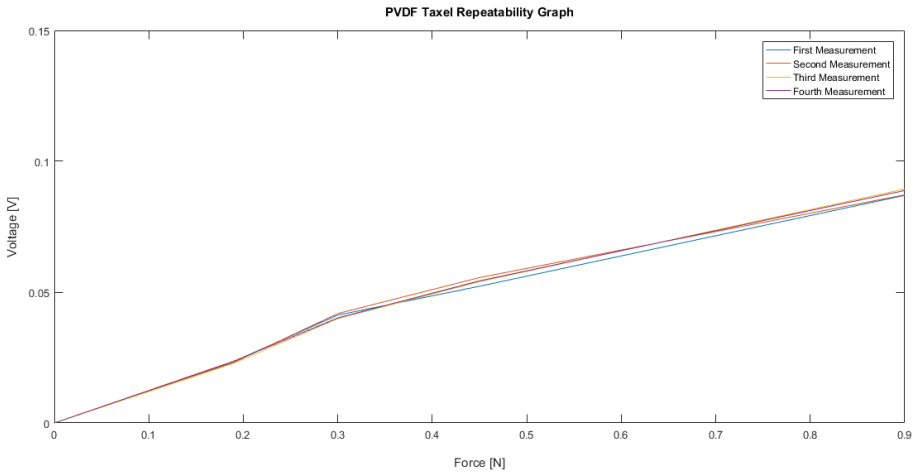

Figure 4.18 : Repeatability graph of PVDF taxel.

4.3.5 Silicone thickness effect analysis

In this section the effect of silicone layer on voltage output of the taxel has been experimented. The taxels used in previous sections are embedded in silicone. At each stage two layers of 4x4 mm silicone with thickness of 0.5 mm is attached to bottom and top surfaces of taxel. In the other words, the frequency response of taxel with total silicone thickness 0, 1 and 2 are obtained. As it can be seen from Figures 4.19 and 4.20, silicone layer decreases the voltage output of piezoelectric taxels. However, by increasing the thickness of silicone from 1 mm to 2 mm, the voltage output of the taxels increases which is compatible with FEM analysis. (Figure 2.5)

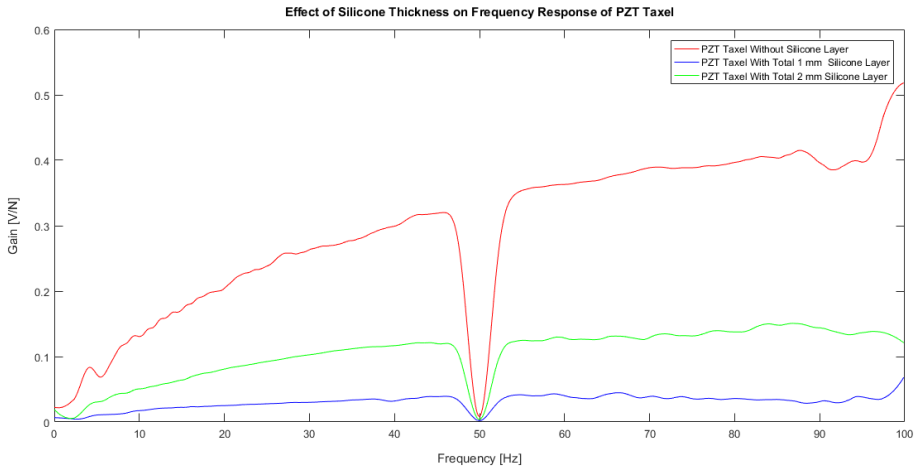

Figure 4.19 : Effect of silicone thickness on the PZT taxel sample.

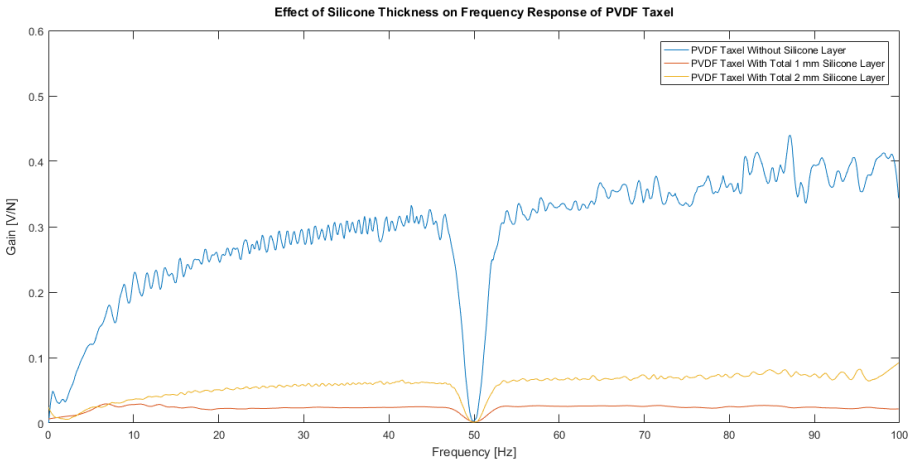

Figure 4.20 : Effect of silicone thickness on the PVDF taxel sample.

4.3.6 Comparison of the results

At this section, the frequency response of theoretical and FEM model of taxels are compared with experiments. Since the charge, capacitance and resistance coefficients of each taxels are different from each other, these parameters should be updated in both theoretical and FEM models for each taxels. Figure 4.21 demonstrates the FEM, theoretical and experimental frequency response of a PZT taxel. Since 50 Hz band stop filter is utilized during the experiments, this filter is applied to the the frequency response of the models. The root mean square error of theoretical and FEM models for both types of PZT and PVDF based taxels are calculated as 9.75% and 11.58% respectively. It should be noted that there are measurement errors during measurement such as movement of the sensors due to vibration of the experimental setup or mains hum noises which affected the results. By decreasing the effect of these noises, the amount of error can be lowered.

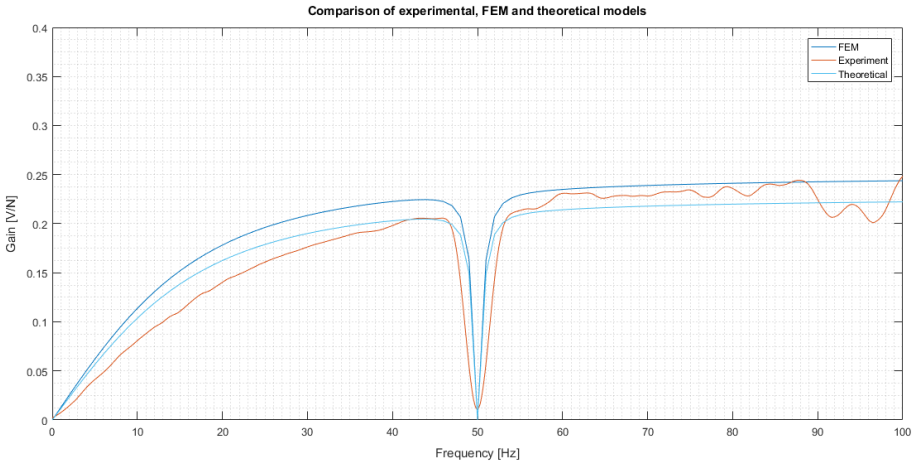

Figure 4.21 : Comparison of experimental, FEM and theoretical models.

4.3.7 Localization of the forces

Localization the place of applied force is one of the tasks defined for the sensors. with help of data obtained form each taxel, the ability of sensor to estimate the position of applied force has been studied. In this section, with help of Labview program, the output voltage of each taxel is measured (Figure 4.22) .Figure4.23 shows the block diagram of this measurement. When there is no applied force, all the led are black. However, when a force is applied on a taxel, a positive peak will be appeared on the output signal of taxels. The taxels with higher value is the taxel closest to the applied force area. It should be noted that in order to estimate force, the all taxels should be calibrated by help of the previous section analysis and force sensor. It has been observed that both PZT and PVDF are capable of localizing force. However, PZT is more sensitive and its correct force localization rate is higher than PVDF one.

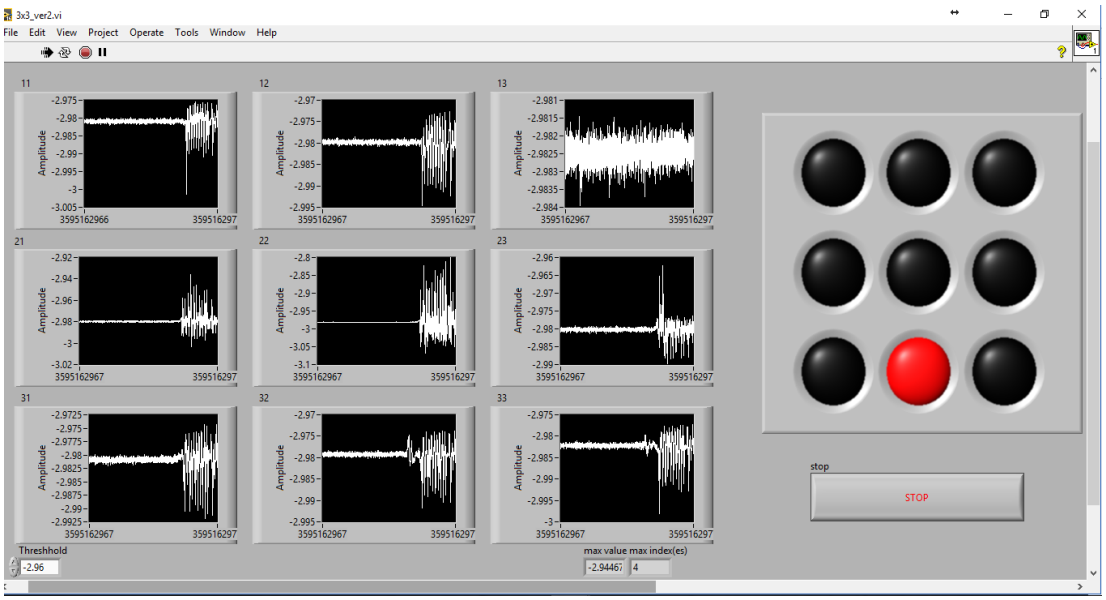

Figure 4.22 : Force localization application of tactile sensor.

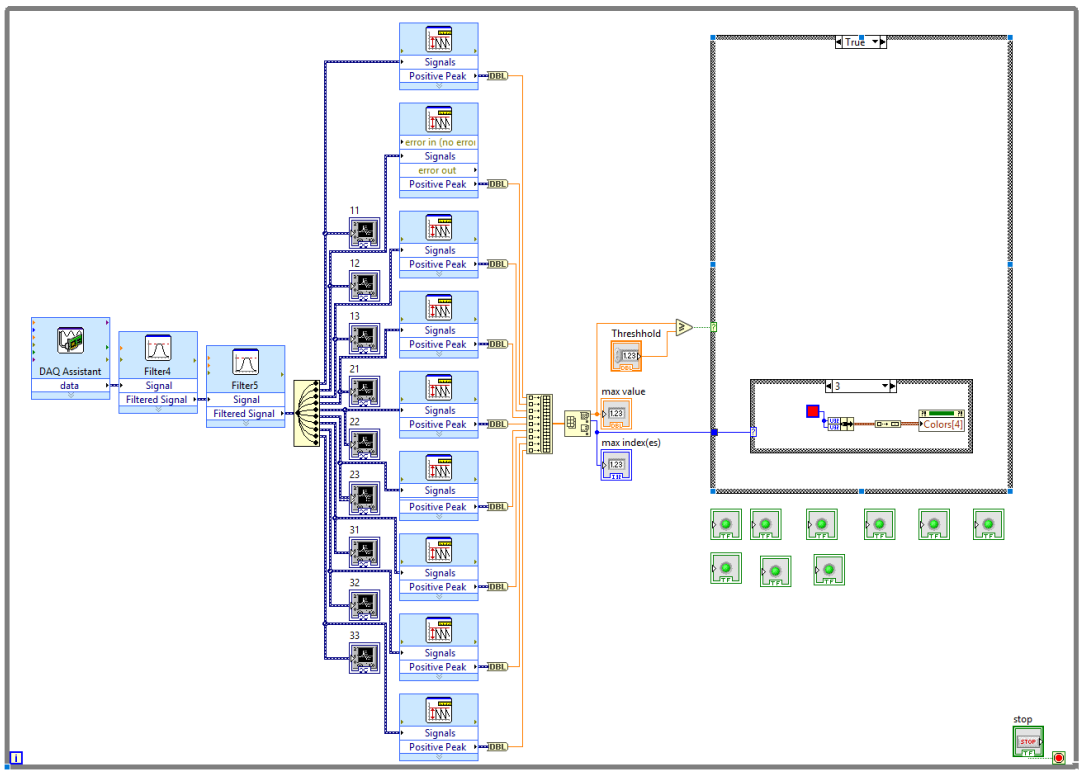

Figure 4.23 : Block diagram of force localization application of tactile sensor.

5. CONCLUSION AND DISCUSSION

The need of designing tactile sensors for machines and robotic systems has become crucial with the increase of the tasks related to human. This thesis proposes two silicone embedded, low profile piezoelectric sensor matrix that is suitable for applications where tactile sensing and force localization is needed. These two tactile sensors are different in the sensing element material and in this project, the characteristic behavior of the sensors in terms of force sensitivity, flexibility and force localization have been compared. The proposed sensors are composed of 9 piezoelectric taxels (PZT or PVDF) placed in the 3x3 array and consisted of 5 layers including flexible electrodes and silicone layers. Taxels are the units of tactile sensing and likewise mechanoreceptors in human skin, they are responsible for touch sensing in tactile sensors.

There are different sensing technologies used in tactile sensing such as capacitive, piezoresistive, optical and piezoelectric based sensors. Even though the high sensitivity, static force measurement ability and acceptable frequency response of capacitive based tactile sensors, these types of sensors have problems such as crosstalk noises, field interactions. Piezoresistive type tactile sensors are another type of tactile sensors. These sensors are preferred due to their structure simplicity and high detection range. Nevertheless, hysteresis and low frequency response are the disadvantages of these sensors. Optical based tactile sensors have wide measurement range, high repeatability. The main drawbacks of these sensors are related to their size and rigidness which causes the inability of embedment and poor wearability. In this project, the piezoelectric material is used due to their good dynamic response and fast time responses. Moreover, the relation between the electric charge induced and the applied mechanical stress is linear.

In order to select the proper design parameters such as silicone thickness and inter-taxel distance, FEM of the sensors have been developed In 2D time dependent analysis, the relationship between silicone thickness and voltage output of the sensor have been obtained. Also, the effect of distance on the voltage output of neighboring taxles has

been calculated. With help of these analyses and the considering the flexibility and wearability, two compact design human inspired tactile sensors have been proposed. As a result of these analyses, the inter taxel distance and the total silicone layer thickness are selected as 3 mm and 2 mm respectively. These sensors are similar in design and manufacturing. However, due to the difference of the proposed tactile sensors in the utilized sensing element, the dynamic response and wearability of them are different.

In this thesis force response properties of the proposed tactile sensors have been investigated. In step response analysis, it has been observed that both piezoelectric sensors, behave as first order system and with the help of this fact time constants of each taxel are calculated. Even if the type of sensing elements are same, the measured time constants for each piezoelectrics are variant. Therefore, each taxel calibrated before using these sensors in force localization and force estimation applications. In addition to step response experiment, impulse response and frequency response of the sensors have experimented. It has been observed that the frequency response of all piezoelectrics are similar to each other.

As it mentioned before, the relation between force and output voltage is linear in the proposed sensors. the correlation coefficient of PZT and PVDF based tactile sensors are respectively 0.9942 and 0.9933 respectively which demonstrate excellent linearity behavior of the proposed sensors.

In addition to these, the force localization ability of the sensors has been investigated. It has been observed that both types of tactile sensors are capable of force localization. PZT based tactile sensors produce more voltage with respect to PVDF one.The reason of this is related to higher piezoelectric coefficient 'd_{ij}' of PZT in comparison to PVDF. Thus, more force sensitive sensors can be produced with the help of PZTs. However, PVDF based tactile sensing is more preferable in wearable technologies because of its high flexibility.

In the third chapter of this thesis, two models have been used in order to estimate the dynamic response of the sensors which are theoretical and FEM models. The results obtained from these models have been compared with experimental results. The root mean square of the error for the theoretical model and FEM model have been calculated as 9.75% and 11.58% respectively. The experimental results are affected by the vibration of the experimental setup and main hum noises. By mounting the

experimental setup on vibration isolation tables, the amount of error could have been decreased

As it mentioned before, piezoelectric based tactile sensors are not able to measure static forces. In order to overcome this problem, additional sensing technologies can be used in the production of the proposed sensors. Besides, the property of piezoelectricity is dependent on the temperature. Therefore, the behavior of the sensor at different temperatures and weather conditions can be investigated. The developed sensors are handmade. By using advanced production technology the production time and sensitivity of the sensors can be enhanced. The proposed tactile sensors are capable of shape recognition and distinguishing between soft and hard materials. The voltage output behavior of the soft materials is different from the hard one. As a future work, with help of machine learning these properties will be investigated. Moreover, the stiffness of materials will be measured and classified as hard and soft materials.

REFERENCES

[1] **Aoyagi, S.**, **Tanaka, T. and Minami, M.** (2006). Recognition of contact state of four layers arrayed type tactile sensor by using neural network, *Information Acquisition, 2006 IEEE International Conference on*, IEEE, pp.393–397.

[2] Pressure Mapping for Automotive Product Design, `https://www.tekscan.com/application-group/test-measurement/automotive`.

[3] TactileSensing, `http://bdml.stanford.edu/Main/TactileSensing`.

[4] (2017), Tactile Feedback Robotic Surgery, `https://www.tekscan.com/applications/tactile-feedback-robotic-surgery`.

[5] **KG, P.I.P.G..C.**, Know-How and Technology, `https://www.physikinstrumente.com/en/technology/piezo-technology/fundamentals/`.

[6] **Jalili, N. and Afshari, M.** (2010). Piezolectric-Based Vibration Control: From Macro to Micro, *Nano Scale Systems, Springer, New York*.

[7] **Karki, J.** *et al.* (2000). Signal conditioning piezoelectric sensors, *App. rept. on mixed signal products (sloa033a), Texas Instruments Incorporated*.

[8] **Tiwana, M.I.**, **Redmond, S.J. and Lovell, N.H.** (2012). A review of tactile sensing technologies with applications in biomedical engineering, *Sensors and Actuators A: physical*, *179*, 17–31.

[9] Pressure Mapping, Force Measurement,Tactile Sensors, `https://www.tekscan.com/`.

[10] **Romano, J.M.**, **Hsiao, K.**, **Niemeyer, G.**, **Chitta, S. and Kuchenbecker, K.J.** (2011). Human-inspired robotic grasp control with tactile sensing, *IEEE Transactions on Robotics*, *27*(6), 1067–1079.

[11] **Chuang, C.H.**, **Li, T.H.**, **Chou, I.C. and Teng, Y.J.** (2016). Piezoelectric tactile sensor for submucosal tumor detection in endoscopy, *Sensors and Actuators A: Physical*, *244*, 299–309.

[12] **Sawada, H. and Takeda, Y.** (2015). Tactile pen for presenting texture sensation from touch screen, *Human System Interactions (HSI), 2015 8th International Conference on*, IEEE, pp.334–339.

[13] **Dargahi, J.**, **Sokhanvar, S.**, **Najarian, S. and Arbatani, S.** (2012). *Tactile sensing and display: haptic feedback for minimally invasive surgery and robotics*, John Wiley & Sons.

[14] **Ishizuka, H. and Miki, N.** (2015). MEMS-based tactile displays, *Displays*, *37*, 25–32.

[15] **Girão, P.S.**, **Ramos, P.M.P.**, **Postolache, O. and Pereira, J.M.D.** (2013). Tactile sensors for robotic applications, *Measurement*, *46*(3), 1257–1271.

[16] **Harmon, L.D.** (1982). Automated tactile sensing, *The International Journal of Robotics Research*, *1*(2), 3–32.

[17] **Harmon, L.D.**, (1984). Tactile sensing for robots, Robotics and Artificial Intelligence, Springer, pp.109–157.

[18] **Harmon, L.D.** (1980). Touch-sensing technology- A review, *Society of Manufacturing Engineers, 1980. 58*.

[19] **Lee, M.H.** (2000). Tactile sensing: new directions, new challenges, *The International Journal of Robotics Research*, *19*(7), 636–643.

[20] **Dahiya, R.S.**, **Metta, G.**, **Valle, M. and Sandini, G.** (2010). Tactile sensing—from humans to humanoids, *IEEE Transactions on Robotics*, *26*(1), 1–20.

[21] **Kaufman, C.S.**, **Jacobson, L.**, **Bachman, B.A. and Kaufman, L.B.** (2006). Digital documentation of the physical examination: moving the clinical breast exam to the electronic medical record, *The American journal of surgery*, *192*(4), 444–449.

[22] **Kim, K.**, **Lee, K.R.**, **Kim, W.H.**, **Park, K.B.**, **Kim, T.H.**, **Kim, J.S. and Pak, J.J.** (2009). Polymer-based flexible tactile sensor up to 32$\times$ 32 arrays integrated with interconnection terminals, *Sensors and Actuators A: Physical*, *156*(2), 284–291.

[23] **Lee, H.K.**, **Chung, J.**, **Chang, S.I. and Yoon, E.** (2011). Real-time measurement of the three-axis contact force distribution using a flexible capacitive polymer tactile sensor, *Journal of Micromechanics and Microengineering*, *21*(3), 035010.

[24] **Lipomi, D.J.**, **Vosgueritchian, M.**, **Tee, B.C.**, **Hellstrom, S.L.**, **Lee, J.A.**, **Fox, C.H. and Bao, Z.** (2011). Skin-like pressure and strain sensors based on transparent elastic films of carbon nanotubes, *Nature nanotechnology*, *6*(12), 788–792.

[25] **Park, C.S.**, **Park, J. and Lee, D.W.** (2009). A piezoresistive tactile sensor based on carbon fibers and polymer substrates, *Microelectronic Engineering*, *86*(4), 1250–1253.

[26] **Hasegawa, Y.**, **Shikida, M.**, **Shimizu, T.**, **Miyaji, T.**, **Sasaki, H.**, **Sato, K. and Itoigawa, K.** (2004). Amicromachined active tactile sensor for hardness detection, *Sensors and Actuators A: physical*, *114*(2), 141–146.

[27] **Massaro, A.**, **Spano, F.**, **Missori, M.**, **Malvindi, M.A.**, **Cazzato, P.**, **Cingolani, R. and Athanassiou, A.** (2014). Flexible nanocomposites with all-optical tactile sensing capability, *RSC Advances*, *4*(6), 2820–2825.

[28] **Ohka, M.**, **Mitsuya, Y.**, **Higashioka, I. and Kabeshita, H.** (2005). An experimental optical three-axis tactile sensor for micro-robots, *Robotica*, *23*(4), 457–465.

[29] **Jaffe, B.** (2012). *Piezoelectric ceramics*, volume 3, Elsevier.

[30] **Yi, Z.**, **Zhang, Y. and Peters, J.** (2017). Bioinspired tactile sensor for surface roughness discrimination, *Sensors and Actuators A: Physical*, *255*, 46–53.

[31] **Wan, Y.**, **Wang, Y. and Guo, C.F.** (2017). Recent progresses on flexible tactile sensors, *Materials Today Physics*, *1*, 61–73.

[32] **Hammock, M.L.**, **Chortos, A.**, **Tee, B.C.K.**, **Tok, J.B.H. and Bao, Z.** (2013). 25th anniversary article: the evolution of electronic skin (e-skin): a brief history, design considerations, and recent progress, *Advanced Materials*, *25*(42), 5997–6038.

[33] **Curie, J. and Curie, P.** (1880). Développement, par pression, de l'électricité polaire dans les cristaux hémièdres à faces inclinées, *Comptes rendus*, *91*, 294–295.

[34] **Lippmann, M.** (1881). On the principle of the conservation of electricity.

[35] **Curie, J. and Curie, P.** (1881). Contractions et dilatations produites par des tensions électriques dans les cristaux hémièdres à faces inclinées, *Compt. Rend*, *93*, 1137–1140.

[36] **Zhu, X.** (2010). *Piezoelectric ceramic materials: processing, properties, characterization, and applications*, Nova Science Publ.

[37] **Voigt, W.** (1908). Lehrbuch der Kristallphysik (Teubner, Leipzig, 1928), *MATH Google Scholar*, 716.

[38] **Langevin, P.** (1918). Procédé et appareils d'émission et de réception des ondes élastiques sous-marines à l'aide des propriétés piézoélectriques du quartz, *Brevet d'Invention*, (505,703).

[39] **Sharapov, V.** (2011). *Piezoceramic sensors*, Springer Science & Business Media.

[40] (1996). Publication and Proposed Revision of ANSI/IEEE Standard 176-1987 "ANSI/IEEE Standard on Piezoelectricity", *IEEE Transactions on Ultrasonics, Ferroelectrics, and Frequency Control*, *43*(5), 717–.

[41] **Erturk, A. and Inman, D.J.** (2011). *Piezoelectric energy harvesting*, John Wiley & Sons.

[42] **Sokhanvar, S.**, **Dargahi, J.**, **Najarian, S. and Arbatani, S.** (2013). Piezoelectric Polymers: PVDF Fundamentals, *Tactile Sensing and Displays: Haptic Feedback for Minimally Invasive Surgery and Robotics*, 37–65.

[43] **Sirohi, J. and Chopra, I.** (2000). Fundamental understanding of piezoelectric strain sensors, *Journal of intelligent material systems and structures*, *11*(4), 246–257.

[44] **Fulay, P. and Lee, J.K.** (2016). *Electronic, magnetic, and optical materials*, CRC Press.

[45] Piezo terminology, `http://www.piezo.com/tech1terms.html`.

[46] **Acer, M.**, **Salerno, M.**, **Agbeviade, K. and Paik, J.** (2015). Development and characterization of silicone embedded distributed piezoelectric sensors for contact detection, *Smart Materials and Structures*, *24*(7), 075030.

[47] PSI-5H4E PIEZOCERAMIC SHEETS and their properties, `http://www.piezo.com/prodsheet2sq5H.html`.

[48] **Measurement Specialties, I.** Piezo Film Sensors Technical Manual, Measurement Specialties,Inc., 950 Forge Avenue, Norristown, PA 19403.

[49] **Tong, M.**, (2014), Design, Modeling, and Fabrication of a Massage Neck Support Using Soft Robot Mechanism.

[50] **Atieh, A.**, **Kalantari, M.**, **Ahmadi, R.**, **Dargahi, J.**, **Packirisamy, M. and Zadeh, M.H.** (2011). FEM analysis of the interaction between a piezoresistive tactile sensor and biological tissues, *World Academy of Science, Engineering and Technology, International Journal of Medical, Health, Biomedical, Bioengineering and Pharmaceutical Engineering*, *5*(6), 250–254.

[51] **Yeoh, O.** (1993). Some forms of the strain energy function for rubber, *Rubber Chemistry and technology*, *66*(5), 754–771.

[52] **Ricci, M.**, **Burrascano, P.**, **Carpentieri, M.**, **Tomasello, R. and Finocchio, G.** (2014). Chirp spectroscopy applied to the characterization of Ferromagnetic Resonance in Magnetic Tunnel Junctions, *IEEE Transactions on Magnetics*, *50*(11), 1–5.

CURRICULUM VITAE

Name Surname:
Farshad Hamedi Bazzaz
Place and Date of Birth:
Tehran Iran 07.09.1993
E-Mail:
fb.hamedi@gmail.com

EDUCATION:

- **B.Sc.:** 2016, Istanbul Technical University, Faculty of Mechanics, Mechanical Engineering

PUBLICATIONS, PRESENTATIONS AND PATENTS ON THE THESIS:

- M. Acer, A. F. Yıldız and F. Hamedi Bazzaz, 2017.Development of Soft PZT Based Tactile Sensor Array for Force Localization. *ICAT2017 XXVI International Conference on Information, Communication and Automation Technologies*, October 26-28, 2017 Sarajevo, Bosnia and Herzegovina.